Applied Numerical Mathematics 184 (2023) 18–48

Contents lists available at ScienceDirect

Applied Numerical Mathematics

journal homepage: www.elsevier.com/locate/apnum

Implicit and semi-implicit well-balanced finite-volume methods for systems of balance laws

I. Gómez-Bueno [a,*], S. Boscarino [b], M.J. Castro [a], C. Parés [a], G. Russo [b]

[a] Departamento de Análisis Matemático, Estadística e I.O. y Matemática Aplicada, Facultad de Ciencias, Campus de Teatinos, Universidad de Málaga, 29071 Málaga, Spain
[b] Dipartimento di Matematica ed Informatica, Viale Andrea Doria, 6, 95125, University of Catania, Catania, Italy

ARTICLE INFO

Article history:
Received 12 July 2022
Received in revised form 11 September 2022
Accepted 24 September 2022
Available online 30 September 2022

Keywords:
Systems of balance laws
Well-balanced methods
Finite-volume methods
High-order methods
Reconstruction operators
Implicit methods
Semi-implicit methods
Shallow water equations

ABSTRACT

The aim of this work is to design implicit and semi-implicit high-order well-balanced finite-volume numerical methods for 1D systems of balance laws. The strategy introduced by two of the authors in some previous papers for explicit schemes based on the application of a well-balanced reconstruction operator is applied. The well-balanced property is preserved when quadrature formulas are used to approximate the averages and the integral of the source term in the cells. Concerning the time evolution, this technique is combined with a time discretization method of type RK-IMEX or RK-implicit. The methodology will be applied to several systems of balance laws.

1. Introduction

Numerous physical systems are described by evolutionary partial differential equations which have the structure of hyperbolic systems of balance laws of the form

$$u_t + f(u)_x = S(u)H_x, \tag{1}$$

where

- $u(x,t)$ takes values on an open convex set $\Omega \subset \mathbb{R}^N$;
- $f : \Omega \longrightarrow \mathbb{R}^N$ is the physical flux function;
- the source term is written in the form $S(u)H_x$, where $S : \Omega \longrightarrow \mathbb{R}^N$ and $H : \mathbb{R} \longrightarrow \mathbb{R}$ is a known function.

The system (1) has nontrivial stationary solutions that satisfy the ODE system:

$$f(u)_x = S(u)H_x, \tag{2}$$

* Corresponding author.
E-mail address: igomezbueno@uma.es (I. Gómez-Bueno).

https://doi.org/10.1016/j.apnum.2022.09.016

or

$$J(u)u_x = S(u)H_x,$$

where $J(u)$ is the Jacobian of the flux function. A numerical method is said to be well-balanced if it preserves (in some sense) all or a representative set of steady solutions of (1). The development of numerical schemes satisfying the well-balanced property is a big issue in the simulation of small perturbations of stationary solutions in many geophysical problems, such as the tsunami waves in the ocean. Many authors have already dealt with the design of well-balanced methods: see, for example, [3,17,22,31,30,89,33,41,40,52,51,53,69,56,55,71,72,76,77,80–82,86,87,66,92,65,63,35,67,37,26,43,57,64] and their references. In earlier papers, some of the authors introduced a general procedure to build explicit high-order well-balanced numerical methods whose key was the design of high-order well-balanced reconstruction operators (see [28,48–50]). A reconstruction operator is said to be well-balanced if, when the operator is applied to the cell averages of a stationary solution, the approximations in the cells provided by the operator coincides with the stationary solution. In other words, the reconstruction operator must preserve the steady states. However, in general a standard reconstruction operator is not expected to be well-balanced. In this work, we follow the methodology proposed in [28] to obtain a well-balanced operator from a standard one. The reconstruction procedure to compute the approximation of a function in a cell given its averages in the mesh is the following:

1. Find the stationary solution in the stencil whose average in the cell coincides with the given cell average in that cell.
2. Compute the differences between the cell averages and those of the stationary solution found in the previous step in the stencil. Once these differences are obtained, a standard reconstruction operator is applied to them.
3. The reconstruction operator is given by the sum of the stationary solution found in the first step and the approximation found in the second step point.

Note that the first step of the reconstruction procedure involves solving, in each cell, local nonlinear problems consisting in finding a stationary solution in the stencil with given average in the cells. When the expression of the stationary solutions is not available, these problems become difficult and must be numerically solved (see [48,50]). The procedure outlined above is recalled in Section 2.2.

Once a well-balanced space-semi-discrete method has been designed using this general procedure, in principle implicit or semi-implicit fully discrete methods could be obtained just by using implicit or semi-implicit ODE solvers to discretize in time. Nevertheless, such a strategy would require to solve complex global nonlinear systems in order to compute the numerical solution at time t^{n+1}: in particular, these systems would involve local steady states related to the unknown solution at time t^{n+1}, which is unfeasible from the practical point of view. The aim of this work is to introduce a general framework for the derivation of well-balanced implicit and semi-implicit fully discrete numerical methods in which only well-balanced reconstructions at time t^n have to be computed.

To our knowledge, no general framework to design implicit or semi-implicit well-balanced of schemes has been developed so far. In the case of low-order schemes, some works can be found for finite-volume, finite-difference, finite-element and discontinuous Galerkin methods which only work for particular steady states (mainly zero velocity steady states): see, for instance, [32,44,93,29,90,9,70]. See [25] for well-balanced methods for all the one-dimensional steady states for the shallow-water system. Concerning high-order schemes, finite-difference, discontinuous Galerkin methods and combination of finite-volume/finite-element and finite-volume/finite-difference methods that are well-balanced for particular stationary solutions (mainly zero velocity steady states) are presented, for example, in [19,59,88,42,47].

In the context of semi-implicit numerical schemes, RK-IMEX setting represents a powerful tool for the time discretization of system of the form (1) if such it contains both stiff and non stiff terms. Typical examples are hyperbolic systems with stiff hyperbolic or parabolic relaxation characterized by a relaxation parameter ε, [78,14,15,11,10].

In the hyperbolic to hyperbolic relaxation (HHR) a natural treatment consists in adopting RK-IMEX schemes, in which the relaxation term is treated by an implicit scheme, while the hyperbolic part is treated explicitly [78,14]. On the other hand, in hyperbolic systems with parabolic relaxation (HPR), standard RK-IMEX schemes developed for HHR systems are not appropriate, because the characteristic speeds of the hyperbolic term diverge as the relaxation parameter vanishes. Slightly modified IMEX schemes become consistent discretization of the limit diffusive relaxed system, but suffer from the parabolic CFL restriction. In [15,11,10] this drawback was overcome by a penalization method, so that the limit scheme becomes an implicit scheme for the limit diffusive relaxed system.

Furthermore, in [12] a unified RK-IMEX approach was introduced for systems which may admit both hyperbolic and parabolic relaxation (for example with space dependent relaxation parameter). Thus, this latter approach applies to both HHR and HPR. All these approaches are capable to capture the correct asymptotic limit of the system when $\varepsilon \to 0$, i.e., the schemes are asymptotic preserving (AP) independently of the scaling used.

The organization of the article is as follows: in Section 2 we present an overview to build both exactly well-balanced and well-balanced reconstruction operators and its application to design explicit high-order numerical schemes satisfying this property. Section 3 is devoted to obtain well-balanced implicit methods. We introduce a general procedure to design well-balanced reconstruction operators adapted to implicit methods and a general result is stated showing that well-balanced reconstruction operators lead to well-balanced methods. Section 4 is focused on how the time discretization is performed,

including the particular case of implicit first- and second-order well-balanced schemes. Section 4 ends with the semi-implicit case. In Section 5, numerous numerical tests are performed to check the well-balanced property of the implicit and semi-implicit numerical methods. Even though the introduced strategy can be used to design arbitrary high-order well-balanced methods, only first- and second-order methods have been implemented. We consider numerical tests for scalar and systems of balance laws: the transport equation, the Burgers equation with a non-linear source term and the shallow water model with and without Manning friction. Eventually, some conclusions are drawn in Section 6 and possible forthcoming works are also discussed.

2. Preliminaries

As discussed earlier, in previous works, two of the authors introduced a general procedure to design explicit methods satisfying these properties based on the use of reconstructions operators. This general strategy involves nonlinear problems to be solved at every computational cell and time step consisting in finding a stationary solution of (1) with given average in the cell. If the expression of the stationary solutions if available, exactly well-balanced methods can be designed. If it is not the case, one can obtain methods that are well-balanced.

2.1. Exactly well-balanced methods

Remember that, given the set $\{\overline{u}_i\}$ of cell-averages of a function u

$$\overline{u}_i = \frac{1}{\Delta x}\int_{x_{i-1/2}}^{x_{i+1/2}} u(x)\,dx,$$

or their approximations using a quadrature formula

$$\overline{u}_i = \sum_{m=1}^{M} \alpha_m u(x_i^m),$$

where x_i^m and α_m are, respectively, the nodes and the weights of the quadrature formula, a reconstruction operator provides approximations of u at the cells

$$u(x) \approx P_i(x; \{\bar{u}_j\}_{j\in\mathcal{S}_i\}}, \quad x \in [x_{i-1/2}, x_{i+1/2}],$$

where $x_{i\pm1/2}$ represent the inter-cells. Here for simplicity we assume that space discretization is uniform, so that the weights do not depend on i, and $x_i^m = x_{i-1/2} + c_m\Delta x$, $m = 1,\dots,M$, where c_m denotes the nodes of the quadrature formula in the interval $[0,1]$. These approximations are obtained by interpolation or approximation techniques from the cell values at the cells belonging to the stencil of the ith cell: $\mathcal{S}_i$ represents the set of their indexes. MUSCL, ENO, or CWENO are examples of high-order reconstruction operators. It will be assumed from now on that all the cell-averages are approximated using a fixed quadrature formula.

The design of explicit high-order well-balanced numerical methods discussed in [28] is based on the use of reconstruction operators that are well-balanced according to the following definition:

Definition 1. Given a stationary solution u^e of (1), a reconstruction operator $P_i(x)$ is said to be exactly well-balanced for u^e if

$$P_i(x; \{\overline{u}_j^e\}_{j\in\mathcal{S}_i}) = u^e(x), \quad \forall x \in [x_{i-\frac{1}{2}}, x_{i+\frac{1}{2}}],\ \forall i,$$

where $\overline{u}_j^e$ represent the exact cell-averages or the approximate cell-averages obtained by a quadrature formula from the stationary solution u^e.

Since, in general, a standard reconstruction operator is not expected to be well-balanced, the following strategy introduced in [24] is used to obtain a well-balanced operator P_i from a standard one Q_i:

Algorithm 1. Given a family of cell values $\{\overline{u}_i\}$, at every cell $I_i = [x_{i-1/2}, x_{i+1/2}]$:

1. Find, if it is possible, a stationary solution $u_i^e(x)$ of (1) defined in the stencil of cell I_i such that:

$$\sum_{m=1}^{M} \alpha_m u_i^e(x_i^m) = \overline{u}_i.$$

2. Apply the reconstruction operator to the cell values $\{v_j\}_{j\in\mathcal{S}_i}$ given by

$$v_j = \overline{u}_j - \sum_{m=1}^{M} \alpha_m u_i^e(x_j^m)$$

to obtain

$$Q_i(x) = Q_i(x; \{v_j^n\}_{j\in\mathcal{S}_i}).$$

3. Define

$$P_i(x) = u_i^e(x) + Q_i(x).$$

It can be easily proved that the reconstruction operator P_i is exactly well-balanced provided that Q_i is exact for the zero function. Notice that, at every cell, a nonlinear problem has to be solved in the first step consisting in finding a stationary solution in the stencil of the cell with prescribed average in the cell. Therefore, the expression of the stationary solutions either in explicit or implicit form is required.

Once the exactly well-balanced reconstruction operator has been built, the semi-discrete numerical methods write as follows:

$$\begin{aligned}\frac{du_i}{dt} = &-\frac{1}{\Delta x}\left(F_{i+1/2}(t) - F_{i-1/2}(t)\right) + \frac{1}{\Delta x}\left(f\left(u_i^{e,t}(x_{i+1/2})\right) - f\left(u_i^{e,t}(x_{i-1/2})\right)\right)\\ &+ \sum_{m=1}^{M} \alpha_m \left(S(P_i^t(x_i^m)) - S(u_i^{e,t}(x_i^m))\right) H_x(x_i^m),\ \forall i,\end{aligned} \tag{3}$$

where

- P_i^t is the well-balanced reconstruction obtained from the cell values $\{u_i(t)\}$;
- $u_i^{e,t}$ is the stationary solution found at the first step of the reconstruction procedure at the ith cell;
- $F_{i+1/2}(t) = \mathbb{F}(u_{i+1/2}^{t,-}, u_{i+1/2}^{t,+})$, where $\mathbb{F}$ is any consistent numerical flux and

$$u_{i+1/2}^{t,-} = P_i^t(x_{i+1/2}), \quad u_{i+1/2}^{t,+} = P_{i+1}^t(x_{i+1/2}).$$

Notice that in order to use a lighter notation we write $u_i(t)$ in place of $\overline{u}_i(t)$ to denote a semidiscrete approximation of cell average of the solution,

$$\frac{1}{\Delta x}\int_{x_{i-1/2}}^{x_{1+1/2}} u(x,t)\,dx.$$

This numerical method is well-balanced in the sense that, given any stationary solution u^e, the set of cell values $\{\overline{u}_i^e\}$ is an equilibrium of the ODE system (3): see [28].

2.2. Well-balanced methods

When the expression of the stationary solutions in explicit or implicit form is not available, reconstruction operators that are just well-balanced but not exactly well-balanced can be designed following the idea developed in [48–50]: consider a numerical solver of the ODE system (2) that provides approximations of a stationary solution u^e at the inter-cells and the quadrature points

$$u_{i+1/2}^e \approx u^e(x_{i+1/2}), \quad u_{i,m}^e \approx u^e(x_i^m),\ m = 1,\dots,M, \quad \forall i.$$

Well-balanced reconstruction operators are then defined as follows:

Definition 2. Given a stationary solution u^e of (1), a reconstruction operator $P_i(x)$ is said to be well-balanced for u^e if, for every i:

$$\begin{aligned}&P_i(x_{i\pm1/2}; \{\overline{u}_j^e\}_{j\in\mathcal{S}_i}) = u_{i\pm1/2}^e,\\ &P_i(x_i^m; \{\overline{u}_j^e\}_{j\in\mathcal{S}_i}) = u_{i,m}^e,\ m = 1,\dots,M,\end{aligned}$$

where here the cell-averages $\{\overline{u}_i^e\}$ are given by

$$\overline{u}_i^e = \sum_{m=1}^{M} \alpha_m u_{i,m}^e.$$

Algorithm 1 is modified as follows to obtain well-balanced reconstruction operators:

Algorithm 2. Given a family of cell values $\{\overline{u}_i\}$, at every cell $I_i = [x_{i-1/2}, x_{i+1/2}]$:

1. Find, if it is possible, a stationary solution $u_i^e(x)$ of (1) defined in the stencil of cell I_i such that:

$$\sum_{m=1}^{M} \alpha_m u_{i;i,m}^e = \overline{u}_i,$$

where

$$u_{i;i,m}^e \approx u_i^e(x_i^m),\ m = 1, \dots, M,$$

are the approximations provided by the selected numerical solver for (2).

2. Apply the reconstruction operator to the cell values $\{v_j\}_{j\in\mathcal{S}_i}$ given by

$$v_j = \overline{u}_j - \sum_{m=1}^{M} \alpha_m u_{i;j,m}^e$$

to obtain

$$Q_i(x) = Q_i(x; \{v_j^n\}_{j\in\mathcal{S}_i}),$$

where

$$u_{i;j,m}^e \approx u_i^e(x_j^m),\ m = 1, \dots, M, \quad j \in \mathcal{S}_i.$$

3. Define

$$\begin{aligned} u_{i-1/2}^+ &= u_{i;i-1/2}^e + Q_i(x_{i-1/2}),\\ u_{i+1/2}^- &= u_{i;i+1/2}^e + Q_i(x_{i+1/2}),\\ P_i(x_i^m) &= u_{i;i,m}^e + Q_i(x_i^m),\ m = 1, \dots, M, \end{aligned}$$

where

$$u_{i;i\pm1/2}^e \approx u_i^e(x_{i\pm1/2}).$$

Observe that, in order to implement (3) it is enough to compute the reconstructions at the inter-cells and at the quadrature points.

The first step of the reconstruction procedure consists now of applying a numerical solver to the ODE system (2) to find a solution with prescribed average at a cell. Two different strategies have been developed to solve these problems:

- A control-based approach (see [48,49]). The nonlinear problems to be solved in the reconstruction procedure are interpreted as control problems, in which the control is the value of the solution at the left extreme point of the stencil. The gradient of the functional is computed on the basis of the adjoint problem. Different gradient-type methods and the Newton's method are applied to solve the control problems.
- A technique based on RK collocation methods (see [50]). RK collocation methods are used to solve (2) with prescribed average in each cell I_i and to extend the found stationary solution to the cells belonging to stencil $\mathcal{S}_i$.

Once the well-balanced reconstruction operator has been built, the semi-discrete numerical method writes as follows:

$$\begin{aligned} \frac{du_i}{dt} = &-\frac{1}{\Delta x}\left(F_{i+1/2}(t) - F_{i-1/2}(t)\right) + \frac{1}{\Delta x}\left(f\left(u_{i;i+1/2}^{e,t}\right) - f\left(u_{i;i-1/2}^{e,t}\right)\right)\\ &+ \sum_{m=1}^{M} \alpha_m \left(S(P_i^t(x_i^m)) - S(u_{i;i,m}^{e,t})\right) H_x(x_i^m),\ \forall i, \end{aligned} \tag{4}$$

where now $u^{e,t}_{i;i\pm1/2}$, $u^{e,t}_{i;i,m}$ are the approximations at the inter-cells $x_{i\pm1/2}$ and the quadrature points x^m_i of the stationary solution $u^{e,t}_i$ found at the first step of the reconstruction procedure at the ith cell.

This numerical method is well-balanced in the sense that, given any stationary solution u^e, the set of cell values $\{u^e_i\}$ given by

$$u^e_i = \sum_{m=1}^{M} \alpha_m u^e_{i,m}$$

is an equilibrium of the ODE system (4): see [50].

Observe that (3) is the particular case of (4) corresponding to the exact ODE solver for system (2), i.e.

$$u^{e,t}_{i;i\pm1/2} = u^{e,t}_i(x_{i+1/2}),$$
$$u^{e,t}_{i;j,m} = u^{e,t}(x^m_j), \quad m = 1,\dots,M.$$

Therefore, only the expression of the method (4) will be considered without loss of generality.

2.3. Explicit methods

Explicit high-order well-balanced numerical methods are then obtained by applying an ODE solver (usually a TVD RK method) to the ODE systems (3) or (4).

3. Implicit methods

Although in principle implicit high-order well-balanced methods can be obtained by applying implicit ODE solvers to (3) or (4), in practice the well-balanced reconstruction of the unknown solution u^{n+1} would lead to complex nonlinear systems that may be costly to solve. To avoid this we look for a solution of the ODE system in $[t^n, t^{n+1}]$ of the form $u_i(t) = u^n_i + u^f_i(t)$, and adopt besides the standard reconstruction operator Q, a new reconstruction $\tilde{Q}$, which will act on the perturbation u^f_i as described below. Once the approximations at time t^n, $\{u^n_i\}$, have been computed, in order to update them we proceed as follows:

- First, the well-balanced reconstruction procedure is applied to $\{u^n_i\}$ to obtain:

$$P^n_i(x) = u^{e,n}_i(x) + Q_i(x; \{v^n_j\}_{j\in\mathcal{S}_i}),$$

  where $u^{e,n}_i(x)$ is the stationary solution found at the first step of the reconstruction procedure at the ith cell.
- Next we consider the following ODE system in the time interval $[t^n, t^{n+1}]$:

$$\begin{aligned}\frac{du^f_i}{dt} = &-\frac{1}{\Delta x}\left(F_{i+1/2}(t) - F_{i-1/2}(t)\right) + \frac{1}{\Delta x}\left(f\left(u^{e,n}_{i;i+1/2}\right) - f\left(u^{e,n}_{i;i-1/2}\right)\right)\\ &+ \sum_{m=1}^{M}\alpha_m\left(S(P^t_i(x^m_i)) - S(u^{e,n}_{i;i,m})\right)H_x(x^m_i),\ \forall i,\end{aligned} \tag{5}$$

  with initial condition

$$u^f_i(t^n) = 0, \quad \forall i.$$

  Here

$$P^t_i(x) = P^n_i(x) + \widetilde{Q}_i(x; \{u^f_j\}_{j\in\widetilde{\mathcal{S}}_i}), \tag{6}$$

  and

$$F_{i+1/2}(t) = \mathbb{F}(u^{t,-}_{i+1/2}, u^{t,+}_{i+1/2}), \tag{7}$$

  where

$$u^{t,-}_{i+1/2} = P^t_i(x_{i+1/2}), \quad u^{t,+}_{i+1/2} = P^t_{i+1}(x_{i+1/2}). \tag{8}$$

- Define:

$$u^{n+1}_i = u^n_i + u^f_i(t^{n+1}). \tag{9}$$

Observe that, although

$$u_i(t) = u_i^n + u_i^f(t), \quad t \in [t^n, t^{n+1}]$$

formally solves (4), the reconstruction P_i^t is not the same as the one in the previous section: while there one had

$$P_i^t(x) = u_i^{e,t}(x) + Q_i(x; \{v_j\}_{j\in\mathcal{S}_i}),$$

now,

$$P_i^t(x) = u_i^{e,n}(x) + Q_i(x; \{v_j^n\}_{j\in\mathcal{S}_i}) + \widetilde{Q}_i(x; \{u_j^f(t)\}_{j\in\widetilde{\mathcal{S}}_i}).$$

The main differences are the following:

- to compute P_i^t the stationary solution $u_i^{e,n}$ is used instead of $u_i^{e,t}$;
- the reconstruction operator $\widetilde{Q}_i$ will be in practice easier and cheaper to compute than Q_i: in particular, the smoothness indicators obtained to compute Q_i at time t^n may be used to compute $\widetilde{Q}_i$. We shall require that $\widetilde{Q}_i$ maintains null states and its order of accuracy is p.

The description of the fully discrete schemes will be completed in the next section, by specifying how to solve the ODE system (5)-(9).

Some properties of the numerical schemes do not depend on the detail of the particular scheme that is adopted for the numerical solution of system (5)-(9), therefore we shall discuss them in this section.

3.1. Well-balanced property

Here we state two results concerning the well-balanced properties of the schemes described at the beginning of the section.

Theorem 1. *Given a stationary solution u^e of (1), let us suppose that, at every cell, at every time step, P_i^n is a well-balanced reconstruction operator. Then, the numerical method (9) is well-balanced for u^e, in the sense that, if the initial condition is given by*

$$u_i^0 = \sum_{m=1}^{M} \alpha_m u_{i,m}^e,$$

then

$$u_i^n = u_i^0$$

for every n and every i.

The proof is straightforward: it is enough to check that at every cell, at every time step, $u_i^f(t) \equiv 0$ is the solution of the Cauchy problem (5). As a corollary we have:

Theorem 2. *Given a stationary solution u^e of (1), let us suppose that, at every cell, at every time step, P_i^n is an exactly well-balanced reconstruction operator. Then, the numerical method (9) is exactly well-balanced for u^e, in the sense that, if the initial condition is given by*

$$u_i^0 = \sum_{m=1}^{M} \alpha_m u^e(x_i^m),$$

then

$$u_i^n = u_i^0$$

for every n and every i.

4. Time discretization

This section is devoted to time discretization. If system (5)-(9) is not *stiff*, i.e. if accuracy and stability restrictions on the time step Δt are of the same order of magnitude, then one can adopt explicit schemes. This is often the case for hyperbolic systems of balance laws if one is interested in resolving all the waves of the system, i.e. if all the signals transported by the various waves are not negligible, and if the time scales associated to the right hand side are not too small. In such cases one can adopt explicit schemes such as explicit Runge-Kutta of multistep methods. In particular, strongly stability preserving schemes are generally adopted for the numerical solution of hyperbolic systems of balance laws, since they prevent formation of spurious oscillations due to time discretization (see [54]). The literature on well-balanced schemes based on explicit schemes is too vast to mention it here. We just recall the following review papers [28,85,6,46,56,55,71,52,51,53,45,7,8,41,40,87,81,3,17,27,18,69,60,72,68,38,89,21,36,23,24,76,77,86,5,65,92,91,79,75,20,33,58,84,1,83]. For this reason in this paper we do not consider well-balanced schemes based on explicit time discretization methods. The choice of the method adopted for time discretization depends on the problem we want to solve. We shall consider three different situations:

1. only a source term or part of it is stiff while the hyperbolic term is non stiff;
2. the source or part of it and some part of the hyperbolic term are stiff;
3. both the hyperbolic term and the source are stiff and require implicit solver.

Conceptually, the simplest case is the third one, which requires an implicit treatment of both source and the hyperbolic term, so this is the case we start with. In such case one could adopt an implicit scheme for the treatment of (5). Most commonly used implicit Runge-Kutta schemes are the so called diagonally implicit schemes (DIRK), and in particular *singly diagonally implicit* which are described by the following Butcher tableau

$$\begin{array}{c|ccccc} \gamma & \gamma & 0 & 0 & \dots & 0 \\ c_2 & a_{2,1} & \gamma & 0 & \dots & 0 \\ c_3 & a_{3,1} & a_{3,2} & \gamma & \dots & 0 \\ \vdots & \vdots & \vdots & \vdots & \ddots & \vdots \\ 1 & a_{s,1} & a_{s,2} & a_{s,3} & \dots & \gamma \\ \hline & a_{s,1} & a_{s,2} & a_{s,3} & \dots & \gamma \end{array} \tag{10}$$

will be applied to solve the Cauchy problems satisfied by the time fluctuations $u_i^f(t)$:

$$\begin{aligned} u_i^{f,k} &= \Delta t \sum_{l=1}^{k-1} a_{k,l} L_i^l + \Delta t \gamma L_i^k, \quad k = 1, \dots, s, \\ u_i^{f,n+1} &= u_i^{f,s}, \end{aligned}$$

where

$$\begin{aligned} L_i^k = &-\frac{1}{\Delta x}\left(F_{i+1/2}^k - F_{i-1/2}^k\right) + \frac{1}{\Delta x}\left(f\left(u_{i;i+1/2}^{e,n}\right) - f\left(u_{i;i-1/2}^{e,n}\right)\right) \\ &+ \sum_{m=1}^{M} \alpha_m \left(S(P_i^k(x_i^m)) - S(u_{i;i,m}^{e,n})\right) H_x(x_i^m), \; k = 1, \dots, s, \end{aligned} \tag{11}$$

with obvious notation, that can be written as well in the form:

$$\begin{aligned} u_i^{f,k} &= \sum_{l=1}^{k-1} \gamma_{k,l} u_i^{f,l} + \gamma \Delta t L_i^k, \quad k = 1, \dots, s, \\ u_i^{f,n+1} &= u_i^{f,s}, \end{aligned}$$

for some coefficients $\gamma_{k,l}$. The choice of the particular DIRK scheme depends on the problem. If the systems we want to solve are very stiff, then it is advisable to adopt a L-stable scheme, which is the type of schemes we shall use in this paper.

4.1. First-order schemes

The backward Euler method is used to discretize in time. The system for the time fluctuations writes thus as follows:

$$\begin{aligned} u_i^{f,n+1} = &-\frac{\Delta t}{\Delta x}\left(F_{i+1/2}^{n+1} - F_{i-1/2}^{n+1}\right) + \frac{1}{\Delta x}\left(f\left(u_{i;i+1/2}^{e,n}\right) - f\left(u_{i;i-1/2}^{e,n}\right)\right) \\ &+ \Delta t \left(S(P_i^{n+1}(x_i)) - S(u_{i;i}^{e,n})\right) H_x(x_i), \end{aligned} \tag{12}$$

where the midpoint rule has been used to approximate the integrals. The reconstruction operators Q_i and $\widetilde{Q}_i$ are the trivial piecewise constant ones so that:

$$P_i^n(x) = u_i^{e,n}(x), \quad P_i^{n+1} = u_i^{e,n}(x) + u_i^{f,n+1},$$

and therefore the reconstructed states are defined as follows:

$$\begin{cases} u_{i+\frac{1}{2}}^{n+1,-} = u_{i;i+\frac{1}{2}}^{e,n} + u_i^{f,n+1} = u_{i+\frac{1}{2}}^{n,-} + u_i^{f,n+1}, \\ u_{i+\frac{1}{2}}^{n+1,+} = u_{i+1;i+\frac{1}{2}}^{e,n} + u_{i+1}^{f,n+1} = u_{i+\frac{1}{2}}^{n,+} + u_{i+1}^{f,n+1}. \end{cases}$$

Once System (12) has been solved, the cell-averages are updated as follows

$$u_i^{n+1} = u_i^n + u_i^{f,n+1}.$$

Notice that, except for the case of a linear problem, the system to be solved to compute the time fluctuations $u_i^{f,n+1}$, (12), is nonlinear: a numerical method such as a fixed-point algorithm or the Newton's method will be applied to solve them.

4.2. Second-order schemes

The second-order implicit Runge-Kutta method whose Butcher tableau is

$$\begin{array}{c|cc} \gamma & \gamma & 0 \\ 1 & 1-\gamma & \gamma \\ \hline & 1-\gamma & \gamma, \end{array} \tag{13}$$

where $\gamma = 1 - \frac{1}{\sqrt{2}}$, will be used now for the time discretization. Since the scheme is *stiffly accurate*, i.e. $a_{s,i} = b_i$, $i = 1, \dots, s$, then the numerical solution coincides with the last stage value. Then, the fully discrete numerical method is as follows:

$$\begin{aligned} u_i^{f,1} &= \Delta t \gamma L_i^1, \\ u_i^{f,2} &= \Delta t (1-\gamma) L_i^1 + \Delta t \gamma L_i^2, \\ u_i^{f,n+1} &= u_i^{f,2}, \end{aligned} \tag{14}$$

where

$$\begin{aligned} L_i^k = &-\frac{1}{\Delta x}\left(F_{i+1/2}^k - F_{i-1/2}^k\right) + \frac{1}{\Delta x}\left(f\left(u_{i;i+1/2}^{e,n}\right) - f\left(u_{i;i-1/2}^{e,n}\right)\right) \\ &+ \left(S(P_i^k(x_i)) - S(u_{i;i}^{e,n})\right) H_x(x_i), \ k = 1, 2. \end{aligned} \tag{15}$$

Again, the midpoint rule is applied to approximate the integrals and $u_i^{e,n}(x)$ is the stationary solution such that $u_i^{e,n}(x_i) \approx u_{i;i}^{e,n} = u_i^n$.

Since

$$L_i^1 = \frac{u_i^{f,1}}{\Delta t \gamma},$$

(14) can be equivalently written as

$$\begin{aligned} u_i^{f,1} &= \Delta t \gamma L_i^1, \\ u_i^{f,n+1} &= \frac{(1-\gamma)}{\gamma} u_i^{f,1} + \Delta t \gamma L_i^{n+1}, \end{aligned} \tag{16}$$

where the superindex 2 has been replaced by $n+1$, since $u_i^{f,n+1} = u_i^{f,2}$.

The well-balanced reconstruction operator $P_i^n(x)$ is computed on the basis of a MUSCL-type reconstruction operator using three-point stencils

$$\mathcal{S}_i = \{i-1, i, i+1\}$$

as follows:

Algorithm 3. Given the approximations $\{u_i^n\}$ at time t^n:

1. Find, if possible, a stationary solution $u_i^{e,n}(x)$ such that

$$u_{i;i}^{e,n} = u_i^n,$$

where

$$u_{i;i}^{e,n} \approx u_i^e(x_i).$$

2. Apply the second-order reconstruction operator Q_i to $\{v_j^n\}_{j\in\mathcal{S}_i}$ given by

$$v_j^n = u_j^n - u_{i;j}^{e,n}, \quad j \in \mathcal{S}_i,$$

where

$$u_{i;j}^{e,n} \approx u_i^e(x_j), \in \mathcal{S}_i,$$

to obtain

$$Q_i^n(x) = Q_i^n(x; \{v_j^n\}_{j\in\mathcal{S}_i}) = \Delta_i v^n(x - x_i).$$

Here, $\Delta_i v^n$ is a slope limiter, such as the minmod limiter,

$$\Delta_i v^n = \text{minmod}\left(\frac{v_{i+1}^n - v_i^n}{\Delta x}, \frac{v_i^n - v_{i-1}^n}{\Delta x}\right), \tag{17}$$

where

$$\text{minmod}(a,b) = \begin{cases} \min(a,b) & if\ a>0, b>0, \\ \max(a,b) & if\ a<0, b<0, \\ 0 & otherwise, \end{cases} \tag{18}$$

or the avg limiter:

$$\Delta_i v^n = \text{avg}\left(\frac{v_{i+1}^n - v_i^n}{\Delta x}, \frac{v_i^n - v_{i-1}^n}{\Delta x}\right), \tag{19}$$

where

$$\text{avg}(a,b) = \begin{cases} \dfrac{|a|b + |b|a}{|a| + |b|} & if\ |a| + |b| > 0, \\ 0 & otherwise. \end{cases} \tag{20}$$

3. Define

$$u_{i-1/2}^{n,+} = u_{i;i-1/2}^{e,n} + Q_i^n(x_{i-1/2}) = u_{i;i-1/2}^{e,n} - \frac{1}{2}\Delta_i v^n,$$
$$u_{i+1/2}^{n,-} = u_{i;i+1/2}^{e,n} + Q_i^n(x_{i+1/2}) = u_{i;i+1/2}^{e,n} + \frac{1}{2}\Delta_i v^n,$$
$$P_i^n(x_i) = u_{i;i}^{e.n} + Q_i^n(x_i) = u_{i;i}^{e,n},$$

where

$$u_{i;i\pm1/2}^{e,n} \approx u_i^e(x_{i\pm1/2}).$$

Finally, two different choices for $\widetilde{Q}_i^k$ are considered: the trivial piecewise constant reconstruction and a piecewise linear one that uses the slope limiters of P_i^n.

4.2.1. Piecewise constant reconstruction

In this case, $\widetilde{\mathcal{S}}_i = \{i\}$ and the reconstruction operator is given by

$$\widetilde{\mathrm{Q}}_i^k(x) = u_i^{f,k}.$$

With this definition one has:

$$\begin{aligned}
u_{i+1/2}^{k,-} &= u_{i+1/2}^{n,-} + \widetilde{\mathrm{Q}}_i^k(x_{i+1/2}) = u_{i+1/2}^{n,-} + u_i^{f,k},\\
u_{i-1/2}^{k,+} &= u_{i-1/2}^{n,+} + \widetilde{\mathrm{Q}}_i^k(x_{i-1/2}) = u_{i-1/2}^{n,+} + u_i^{f,k},\\
P_i^k(x_i) &= P_i^n(x_i) + \widetilde{\mathrm{Q}}_i^k(x_i) = u_{i;i}^{e,n} + u_i^{f,k}.
\end{aligned}$$

Theorem 3. *Let us suppose that $\widetilde{\mathrm{Q}}_i$ is the piecewise constant reconstruction operator. Then*

$$P_i^t(x) = P_i^n(x) + \widetilde{\mathrm{Q}}_i$$

is a second-order reconstruction operator.

Proof. Given a function $u(x,t)$, we consider the reconstruction operator

$$P_i^t(x) = P_i^n(x) + \overline{u}_i(t) - \overline{u}_i^n,$$

where $\overline{u}_i(t)$ and $\overline{u}_i^n$ represent the cell-averages of u at the i-th cell at times t and t^n, respectively, and P_i^n is a second-order well-balanced reconstruction operator applied to $\{\overline{u}_i^n\}$.

Let us see that P_i^t is a second-order reconstruction operator: given $x \in I_i$ and assuming that $\Delta t = O(\Delta x)$ we have

$$\begin{aligned}
P_i^t(x) &= P_i^n(x) + \overline{u}_i(t) - \overline{u}_i^n\\
&= u(x,t^n) + u(x_i,t) - u(x_i,t^n) + O(\Delta x^2)\\
&= u(x,t^n) + u(x,t^n) + \partial_x u(x,t^n)(x_i - x) + \partial_t u(x,t^n)(t - t^n)\\
&\quad - u(x,t^n) - \partial_x u(x,t^n)(x_i - x) + O(\Delta x^2)\\
&= u(x,t^n) + \partial_t u(x,t^n)(t - t^n) + O(\Delta x^2)\\
&= u(x,t) + O(\Delta x^2).
\end{aligned}$$

Then, P_i^t is second-order accurate. □

4.2.2. Piecewise linear reconstruction operator

In this case, $\widetilde{\mathcal{S}}_i = \mathcal{S}_i = \{i-1, i, i+1\}$ and the reconstruction operator is given by

$$\widetilde{\mathrm{Q}}_i^k(x) = u_i^{f,k} + \Delta u_i^{f,k}(x - x_i),$$

where

$$\Delta u_i^{f,k} = \varphi_i^{n,L}\frac{\left(u_i^{f,k} - u_{i-1}^{f,k}\right)}{\Delta x} + \varphi_i^{n,R}\frac{\left(u_{i+1}^{f,k} - u_i^{f,k}\right)}{\Delta x}.$$

Here, $\varphi_i^{n,L}$ and $\varphi_i^{n,R}$ are two slope limiters computed using the approximations u_i^n at time t^n. For instance, if the avg limiter is chosen, one has:

$$\varphi_i^{n,L} = \frac{|d_R|}{|d_L| + |d_R|}, \quad \varphi_i^{n,R} = \frac{|d_L|}{|d_L| + |d_R|}, \tag{21}$$

where

$$d_L = u_i^n - u_{i-1}^n, \quad d_R = u_{i+1}^n - u_i^n. \tag{22}$$

With this definition one has:

$$\begin{aligned}
u_{i+1/2}^{k,-} &= u_{i+1/2}^{n,-} + \widetilde{\mathrm{Q}}_i^k(x_{i+1/2}) = u_{i+1/2}^{n,-} + u_i^{f,k},\\
u_{i-1/2}^{k,+} &= u_{i-1/2}^{n,+} + \widetilde{\mathrm{Q}}_i^k(x_{i-1/2}) = u_{i-1/2}^{n,+} + u_i^{f,k},\\
P_i^k(x_i) &= P_i^n(x_i) + \widetilde{\mathrm{Q}}_i^k(x_i) = u_{i;i}^{e,n} + u_i^{f,k}.
\end{aligned}$$

where

$$\widetilde{Q}_i^k(x_{i-1/2}) = u_i^{f,k} - \frac{1}{2}\varphi_i^{n,L}\left(u_i^{f,k} - u_{i-1}^{f,k}\right) - \frac{1}{2}\varphi_i^{n,R}\left(u_{i+1}^{f,k} - u_i^{f,k}\right), \tag{23}$$

$$\widetilde{Q}_i^k(x_{i+1/2}) = u_i^{f,k} + \frac{1}{2}\varphi_i^{n,L}\left(u_i^{f,k} - u_{i-1}^{f,k}\right) + \frac{1}{2}\varphi_i^{n,R}\left(u_{i+1}^{f,k} - u_i^{f,k}\right). \tag{24}$$

4.3. Semi-implicit methods

If not all terms of the equation are stiff, then it is not necessary to use a fully implicit scheme for the whole system. Let us suppose, for example, that the problem writes as follows:

$$u_t + f^1(u)_x + f^2(u)_x = S^1(u)H_x + S^2(u), \tag{25}$$

where H is a known function, with f^1 and S^1 non stiff, and f^2 and S^2 stiff. Then the problem can be more efficiently treated by adopting IMEX methods, in which the non stiff terms are treated explicitly, while the stiff terms are treated implicitly. We select numerical fluxes $F^i(u_l, u_r)$, $i = 1, 2$ consistent with f^i, $i = 1, 2$ and an IMEX method with Butcher tableaux:

$$\begin{array}{c|cccccc} 0 & 0 & 0 & 0 & \dots & 0 \\ \tilde{c}_2 & \tilde{a}_{2,1} & 0 & 0 & \dots & 0 \\ \tilde{c}_3 & \tilde{a}_{3,1} & \tilde{a}_{3,2} & 0 & \dots & 0 \\ \vdots & \vdots & \vdots & \vdots & \ddots & \vdots \\ \tilde{c}_s & \tilde{a}_{s,1} & \tilde{a}_{s,2} & \tilde{a}_{s,3} & \dots & 0 \\ \hline & \tilde{b}_1 & \tilde{b}_2 & \tilde{b}_3 & \dots & \tilde{b}_s \end{array}, \qquad \begin{array}{c|cccccc} \gamma & \gamma & 0 & 0 & \dots & 0 \\ c_2 & a_{2,1} & \gamma & 0 & \dots & 0 \\ c_3 & a_{3,1} & a_{3,2} & \gamma & \dots & 0 \\ \vdots & \vdots & \vdots & \vdots & \ddots & \vdots \\ 1 & a_{s,1} & a_{s,2} & a_{s,3} & \dots & \gamma \\ \hline & a_{s,1} & a_{s,2} & a_{s,3} & \dots & \gamma \end{array} \tag{26}$$

The numerical method writes then as follows:

$$\begin{aligned} u_i^{f,k} &= \Delta t \sum_{l=1}^{k-1} \tilde{a}_{k,l} L_i^{1,l} + \Delta t \sum_{l=1}^{k-1} a_{k,l} L_i^{2,l} + \Delta t \gamma L_i^{2,k}, \quad k = 1, \dots, s, \\ u_i^{f,n+1} &= \Delta t \sum_{l=1}^{s} \tilde{b}_i L_i^{1,l} + \Delta t \sum_{l=1}^{s-1} a_{s,i} L_i^{2,l} + \Delta t \gamma L_i^{2,s}, \end{aligned}$$

where

$$\begin{aligned} L_i^{1,k} &= -\frac{1}{\Delta x}\left(F_{i+1/2}^{1,k} - F_{i-1/2}^{1,k}\right) + \frac{1}{\Delta x}\left(f^1\left(u_{i;i+1/2}^{e,n}\right) - f^1\left(u_{i;i-1/2}^{e,n}\right)\right) \\ &\quad + \sum_{m=1}^{M} \alpha_m \left(S^1(P_i^k(x_i^m)) - S^1(u_{i;i,m}^{e,n})\right) H_x(x_i^m); \\ L_i^{2,k} &= -\frac{1}{\Delta x}\left(F_{i+1/2}^{2,k} - F_{i-1/2}^{2,k}\right) + \frac{1}{\Delta x}\left(f^2\left(u_{i;i+1/2}^{e,n}\right) - f^2\left(u_{i;i-1/2}^{e,n}\right)\right) \\ &\quad + \sum_{m=1}^{M} \alpha_m \left(S^2(P_i^k(x_i^m)) - S^2(u_{i;i,m}^{e,n})\right); \end{aligned} \tag{27}$$

for $k = 1, \dots, s$. For instance, if the second order IMEX method with tableaux

$$\begin{array}{c|cc} 0 & 0 & 0 \\ \frac{1}{2\gamma} & \frac{1}{2\gamma} & 0 \\ \hline & 1-\gamma & \gamma \end{array}, \qquad \begin{array}{c|cc} \gamma & \gamma & 0 \\ 1 & 1-\gamma & \gamma \\ \hline & 1-\gamma & \gamma \end{array}, \tag{28}$$

with $\gamma = (2 - \sqrt{2})/2$ is selected, the numerical method writes as follows:

$$\begin{aligned} u_i^{f,1} &= \Delta t \gamma L_i^{2,1}, \\ u_i^{f,2} &= \frac{\Delta t}{2\gamma} L_i^{1,1} + \Delta t (1-\gamma) L_i^{2,1} + \Delta t \gamma L_i^{2,2}, \\ u_i^{f,n+1} &= \Delta t \left((1-\gamma) L_i^{1,1} + \gamma L_i^{1,2} + (1-\gamma) L_i^{2,1} + \gamma L_i^{2,2}\right), \end{aligned}$$

or, equivalently,

$$u_i^{f,1} = \Delta t \gamma L_i^{2,1},$$
$$u_i^{f,2} = \frac{\Delta t}{2\gamma} L_i^{1,1} + \frac{1-\gamma}{\gamma} u_i^{f,1} + \Delta t \gamma L_i^{2,2},$$
$$u_i^{f,n+1} = u_i^{f,2} + \Delta t \left(1 - \gamma - \frac{1}{2\gamma}\right) L_i^{1,1} + \gamma \Delta t L_i^{1,2}.$$

5. Numerical tests

The following acronyms will be used in this section to denote the different methods considered:

- EXWBMp: explicit well-balanced numerical method of order p where the well-balanced reconstruction operator is based on RK collocation methods.
- IEWBMp: implicit exactly well-balanced numerical method of order p.
- IWBMp: implicit well-balanced numerical method of order p where the well-balanced reconstruction operator is based on RK collocation methods.
- SIEWBMp: semi-implicit exactly well-balanced numerical method of order p.
- SIWBMp: semi-implicit well-balanced numerical method of order p where the well-balanced reconstruction operator is based on RK collocation methods.

Although in principle the methodology introduced here can be used to design high-order well-balanced implicit or semi-implicit numerical methods, we have only implemented so far first- and second-order methods. The midpoint rule is considered to approximate the integrals and 1-stage RK collocation methods are applied to obtain the discrete stationary solutions and to solve the local nonlinear problems in the first step of the well-balanced reconstruction procedure.

Since the goal of this work is to introduce a strategy to develop implicit and semi-implicit well-balanced schemes for general systems of balance laws, a wide range of numerical experiments has been performed to check the methods. The scalar balance laws or systems of balance laws considered are the following:

- Linear transport equation with source term.
- Burgers equation with nonlinear source term.
- Shallow water equations without friction.
- Shallow water equations with Manning friction.

In all cases, the following numerical tests are presented to check the well-balanced property of the methods:

- Preservation of a stationary solution: the different numerical methods are run for long time periods starting from a stationary solution to check its preservation.
- Perturbation of a stationary solution: an initial condition that represents a small perturbation of a stationary solution is considered to see how the methods deal with the evolution of the generated waves and how the stationary solution is recovered once the waves have left the computational domain.

Moreover, the accuracy of the methods is checked in three order tests (the transport equation, the Burgers equation and the frictionless shallow water equations). Additionally, two more numerical tests are included in the case of the frictionless shallow water equation to study the shock-capturing property of the methods and the convergence in time of the numerical solutions to a stationary solution starting from an initial condition far from equilibrium.

5.1. Transport equation

Let us consider the linear transport equation

$$u_t + c u_x = \alpha u, \tag{29}$$

where $c, \alpha \in \mathbb{R}$. The stationary solutions of (29) are the 1-parameter family:

$$u^e(x) = C e^{\alpha x / c}, \quad C \in \mathbb{R}.$$

Therefore, given a family of cell averages $\{u_i^n\}$, and considering that cell-averages and pointwise values of a smooth function at cell center agree to second-order in Δx, the stationary solution $u_i^{e,n}(x)$ such that $u_i^{e,n}(x_i) = u_i^n$ is

$$u_i^{e,n}(x) = u_i^n e^{\alpha (x - x_i)/c}.$$

Exactly well-balanced methods will be considered. The Rusanov numerical flux

$$\mathbb{F}(u,v)=\frac{c}{2}(u+v)-\frac{k}{2}(v-u),$$

is considered, with $k=|c|$.

5.1.1. First-order method

In the case of the first-order scheme, one has

$$\begin{aligned}F_{i+1/2}^{n+1}=&\frac{c}{2}\left(u_i^{e,n}(x_{i+1/2})+u_i^{f,n+1}+u_{i+1}^{e,n}(x_{i+1/2})+u_{i+1}^{f,n+1}\right)\\&-\frac{k}{2}\left(u_{i+1}^{e,n}(x_{i+1/2})+u_{i+1}^{f,n+1}-u_i^{e,n}(x_{i+1/2})-u_i^{f,n+1}\right),\end{aligned}$$

which leads to the following expression of (12):

$$\begin{aligned}u_i^{f,n+1}=&-\frac{\Delta t}{\Delta x}\left(\frac{c}{2}\left(u_{i+1}^{f,n+1}-u_{i-1}^{f,n+1}\right)-\frac{k}{2}\left(u_{i+1}^{f,n+1}-2u_i^{f,n+1}+u_{i-1}^{f,n+1}\right)\right)\\&-\frac{\Delta t}{\Delta x}\left(\mathbb{F}\left(u_i^{e,n}(x_{i+1/2}),u_{i+1}^{e,n}(x_{i+1/2})\right)-\mathbb{F}\left(u_{i-1}^{e,n}(x_{i-1/2}),u_i^{e,n}(x_{i-1/2})\right)\right)\\&+\frac{\Delta t}{\Delta x}\left(f\left(u_i^{e,n}(x_{i+1/2})\right)-f\left(u_i^{e,n}(x_{i-1/2})\right)\right)+\alpha\Delta t\left(u_i^{e,n}(x_i)+u_i^{f,n+1}-u_i^{e,n}(x_i)\right).\end{aligned}$$

Since

$$\mathbb{F}\left(u_i^{e,n}(x_{i+1/2}),u_{i+1}^{e,n}(x_{i+1/2})\right)=\mathbb{F}\left(u_{i+1/2}^{n,-},u_{i+1/2}^{n,+}\right)=F_{i+1/2}^{n},$$

the linear system for the time fluctuations for the first-order case is:

$$\begin{aligned}&u_i^{f,n+1}+\frac{\Delta t}{\Delta x}\left(\frac{c}{2}\left(u_{i+1}^{f,n+1}-u_{i-1}^{f,n+1}\right)-\frac{k}{2}\left(u_{i+1}^{f,n+1}-2u_i^{f,n+1}+u_{i-1}^{f,n+1}\right)\right)-\alpha\Delta t u_i^{f,n+1}=\\&\qquad-\frac{\Delta t}{\Delta x}\left(F_{i+1/2}^{n}-F_{i-1/2}^{n}\right)+\frac{\Delta t}{\Delta x}\left(f\left(u_i^{e,n}(x_{i+1/2})\right)-f\left(u_i^{e,n}(x_{i-1/2})\right)\right).\end{aligned}$$

If boundary conditions are neglected, a linear system has to be solved whose matrix is tridiagonal with coefficients

$$d_0=1+\lambda k-\alpha\Delta t,\quad d_{-1}=-\frac{\lambda}{2}(c+k),\quad d_1=-\frac{\lambda}{2}(-c+k),$$

in the main, the lower, and the upper diagonals respectively, where

$$\lambda=\frac{\Delta t}{\Delta x}.$$

5.1.2. Second-order methods

The system of equations for $u_i^{f,1}$ is as follows:

$$\begin{aligned}u_i^{f,1}=&-\frac{\gamma\Delta t}{\Delta x}\left(F_{i+1/2}^{1}-F_{i-1/2}^{1}\right)+\frac{\gamma\Delta t}{\Delta x}\left(f\left(u_i^{e,n}(x_{i+1/2})\right)-f\left(u_i^{e,n}(x_{i-1/2})\right)\right)\\&+\gamma\Delta t\left(u_i^{e,n}(x_i)+u_i^{f,1}-u_i^{e,n}(x_i)\right).\end{aligned}$$

If the piecewise constant reconstruction $\widetilde{Q}_i^k$ described in Subsection 4.2.1 is selected, the expressions of the numerical flux are as follows:

$$\begin{aligned}F_{i+1/2}^{1}=&\frac{c}{2}\left(u_{i+1/2}^{n,-}+u_i^{f,k}+u_{i+1/2}^{n,+}+u_{i+1}^{f,k}\right)\\&-\frac{k}{2}\left(u_{i+1/2}^{n,+}+u_{i+1}^{f,k}-u_{i+1/2}^{n,-}-u_i^{f,k}\right),\end{aligned}$$

and the expression of the numerical method is as follows:

$$\begin{aligned}&u_i^{f,1}+\frac{\gamma\Delta t}{\Delta x}\frac{c}{2}\left(u_{i+1}^{f,1}-u_{i-1}^{f,1}\right)-\frac{\gamma\Delta tk}{2\Delta x}\left(u_{i+1}^{f,1}-2u_i^{f,1}+u_{i-1}^{f,1}\right)-\gamma\alpha\Delta t u_i^{f,1}=\\&\quad-\frac{\gamma\Delta t}{\Delta x}\left(F_{i+1/2}^{n}-F_{i-1/2}^{n}\right)+\frac{\gamma\Delta t}{\Delta x}\left(f\left(u_i^{e,n}(x_{i+1/2})\right)-f\left(u_i^{e,n}(x_{i-1/2})\right)\right).\end{aligned}$$

Table 1
Transport equation: Test 1. L^1-errors at $t = 1, 10, 100, 1000$ for IEWBM1 and IEWBM2 with piecewise constant (PWCR) or piecewise linear (PWLR) reconstruction $\widetilde{Q}_i$.

t	IEWBM1	IEWBM2	
		PWCR	PWLR
1	1.63e-13	1.64e-13	1.57e-13
10	1.63e-13	1.64e-13	1.60e-13
100	1.63e-13	1.63e-13	1.59e-13
1000	1.63e-13	1.63e-13	1.58e-13

$$u_i^{f,n+1} + \frac{\gamma\Delta t}{\Delta x}\frac{c}{2}\left(u_{i+1}^{f,n+1} - u_{i-1}^{f,n+1}\right) - \frac{\gamma\Delta t k}{2\Delta x}\left(u_{i+1}^{f,n+1} - 2u_i^{f,n+1} + u_{i-1}^{f,n+1}\right) - \gamma\alpha\Delta t u_i^{f,n+1} =$$
$$- \frac{\gamma\Delta t}{\Delta x}\left(F_{i+1/2}^n - F_{i-1/2}^n\right) + \frac{\gamma\Delta t}{\Delta x}\left(f\left(u_i^{e,n}(x_{i+1/2})\right) - f\left(u_i^{e,n}(x_{i-1/2})\right)\right) + \frac{1-\gamma}{\gamma}u_i^{f,1}.$$

If, again, boundary conditions are neglected, two linear systems have to be solved with the same tridiagonal matrix whose coefficients are now

$$d_0 = 1 + \gamma\lambda k - \gamma\alpha\Delta t, \quad d_{-1} = -\frac{\gamma\lambda}{2}(c+k), \quad d_1 = -\frac{\gamma\lambda}{2}(-c+k).$$

If we consider now the piecewise linear reconstruction described in Subsection 4.2.2, the implementation of the numerical method (14) leads to solve the following linear systems with pentadiagonal matrices:

$$u_i^{f,1}\left[1 - \gamma\alpha\Delta t + \frac{\gamma\Delta t}{\Delta x}\frac{c}{2}\left(\varphi_i^{n,L} - \varphi_i^{n,R} + \frac{1}{2}\left(\varphi_{i+1}^{n,L} - \varphi_{i-1}^{n,R}\right)\right) + \frac{\gamma\Delta t}{\Delta x}\frac{k}{2}\left(2 - \frac{1}{2}\left(\varphi_{i+1}^{n,L} + \varphi_{i-1}^{n,R}\right)\right)\right]$$
$$+u_{i+1}^{f,1}\left[\frac{\gamma\Delta t}{\Delta x}\frac{c}{2}\left(1 + \varphi_i^{n,R} + \frac{1}{2}\left(\varphi_{i+1}^{n,R} - \varphi_{i+1}^{n,L}\right)\right) - \frac{\gamma\Delta t}{\Delta x}\frac{k}{2}\left(1 + \frac{1}{2}\left(\varphi_{i+1}^{n,R} - \varphi_{i+1}^{n,L}\right)\right)\right]$$
$$+u_{i-1}^{f,1}\left[\frac{\gamma\Delta t}{\Delta x}\frac{c}{2}\left(-1 - \varphi_i^{n,L} + \frac{1}{2}\left(\varphi_{i-1}^{n,R} - \varphi_{i-1}^{n,L}\right)\right) + \frac{\gamma\Delta t}{\Delta x}\frac{k}{2}\left(-1 + \frac{1}{2}\left(\varphi_{i-1}^{n,R} - \varphi_{i-1}^{n,L}\right)\right)\right]$$
$$+u_{i+2}^{f,1}\left[\frac{\gamma\Delta t}{\Delta x}\varphi_{i+1}^{n,R}\frac{k-c}{4}\right] + u_{i-2}^{f,1}\left[\frac{\gamma\Delta t}{\Delta x}\varphi_{i-1}^{n,L}\frac{k+c}{4}\right]$$
$$= -\frac{\gamma\Delta t}{\Delta x}\left(F_{i+1/2}^n - F_{i-1/2}^n\right) + \frac{\gamma\Delta t}{\Delta x}\left(f\left(u_i^{e,n}(x_{i+1/2})\right) - f\left(u_i^{e,n}(x_{i-1/2})\right)\right).$$
$$u_i^{f,n+1}\left[1 - \gamma\alpha\Delta t + \frac{\gamma\Delta t}{\Delta x}\frac{c}{2}\left(\varphi_i^{n,L} - \varphi_i^{n,R} + \frac{1}{2}\left(\varphi_{i+1}^{n,L} - \varphi_{i-1}^{n,R}\right)\right) + \frac{\gamma\Delta t}{\Delta x}\frac{k}{2}\left(2 - \frac{1}{2}\left(\varphi_{i+1}^{n,L} + \varphi_{i-1}^{n,R}\right)\right)\right]$$
$$+u_{i+1}^{f,n+1}\left[\frac{\gamma\Delta t}{\Delta x}\frac{c}{2}\left(1 + \varphi_i^{n,R} + \frac{1}{2}\left(\varphi_{i+1}^{n,R} - \varphi_{i+1}^{n,L}\right)\right) - \frac{\gamma\Delta t}{\Delta x}\frac{k}{2}\left(1 + \frac{1}{2}\left(\varphi_{i+1}^{n,R} - \varphi_{i+1}^{n,L}\right)\right)\right]$$
$$+u_{i-1}^{f,n+1}\left[\frac{\gamma\Delta t}{\Delta x}\frac{c}{2}\left(-1 - \varphi_i^{n,L} + \frac{1}{2}\left(\varphi_{i-1}^{n,R} - \varphi_{i-1}^{n,L}\right)\right) + \frac{\gamma\Delta t}{\Delta x}\frac{k}{2}\left(-1 + \frac{1}{2}\left(\varphi_{i-1}^{n,R} - \varphi_{i-1}^{n,L}\right)\right)\right]$$
$$+u_{i+2}^{f,n+1}\left[\frac{\gamma\Delta t}{\Delta x}\varphi_{i+1}^{n,R}\frac{k-c}{4}\right] + u_{i-2}^{f,n+1}\left[\frac{\gamma\Delta t}{\Delta x}\varphi_{i-1}^{n,L}\frac{k+c}{4}\right]$$
$$= -\frac{\gamma\Delta t}{\Delta x}\left(F_{i+1/2}^n - F_{i-1/2}^n\right) + \frac{\gamma\Delta t}{\Delta x}\left(f\left(u_i^{e,n}(x_{i+1/2})\right) - f\left(u_i^{e,n}(x_{i-1/2})\right)\right) + \frac{1-\gamma}{\gamma}u_i^{f,1}.$$

5.1.3. Test 1: stationary solution

Let us consider the space interval $[0, 2]$ and the time interval $[0, 1000]$, $\alpha = 1$ and $c = 1$. The CFL parameter is set to 2. In order to check the well-balanced property, we consider the stationary solution of (29)

$$u_0(x) = e^x$$

as initial condition. L^1-errors between the initial and final cell-averages have been computed for IEWBMp, $p = 1, 2$, using a 200-cell mesh for different times (see Table 1).

5.1.4. Test 2: perturbation of a stationary solution

We consider now an initial condition that represents a perturbation of the stationary solution of the previous test case:

$$u_0(x) = e^x + \frac{1}{2}e^{-100(x-0.3)^2}.$$

Table 2
Transport equation: Test 2. Differences in L^1-norm between the reference and the numerical solutions and convergence rates at $t = 1$ for IEWBM1 and IEWBM2 with piecewise constant (PWCR) or piecewise linear (PWLR) reconstruction $\widetilde{Q}_i$ with CFL=2.

Cells	IEWBM1		IEWBM2			
			PWCR		PWLR	
	Error	Order	Error	Order	Error	Order
25	7.27e-02	-	3.65e-1	-	1.99e-1	-
50	6.37e-02	0.19	2.72e-01	0.42	1.09e-01	0.87
100	3.83e-02	0.73	1.57e-01	0.79	3.81e-02	1.51
200	2.17e-02	0.82	5.40e-02	1.52	9.39e-03	2.02
400	1.57e-02	0.47	1.45e-02	1.89	2.19e-03	2.10
800	6.62e-03	1.24	3.70e-03	1.98	5.21e-04	2.06
1600	3.43e-03	0.95	9.24e-04	2.00	1.23e-04	2.08

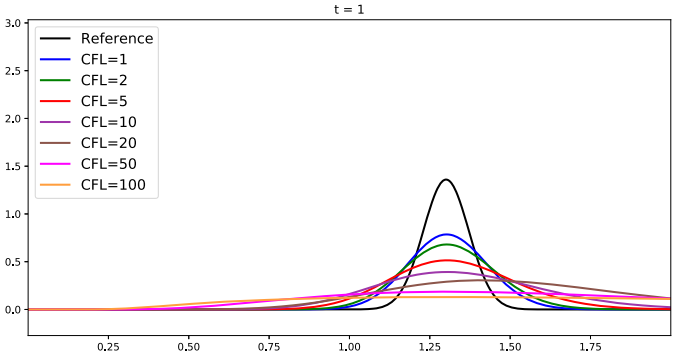

Fig. 1. Transport equation: Test 2. Differences between e^x and the numerical solutions obtained with IEWBM1 using different CFL values at $t = 1$.

Table 3
Transport equation: Test 2. Differences in L^1-norm between the stationary and the numerical solution at $t = 5$ for IEWBM1 and IEWBM2 with piecewise constant (PWCR) or piecewise linear (PWLR) reconstruction $\widetilde{Q}_i$.

IEWBM1	IEWBM2	
	PWCR	PWLR
4.15e-13	4.10e-13	4.09e-13

A reference solution has been obtained using IEWBM2 with piecewise linear reconstruction $\widetilde{Q}_i$ in a 6400-cell mesh. Table 2 shows the errors in L^1-norm with respect to the reference solution for EWBM1 and EWBM2 for both the piecewise constant and linear reconstructions. Notice that the errors decrease with the number of cells at the expected rate.

We have also compared the numerical solutions when different values of the CFL number are chosen (see Figs. 1-2).

Notice that, whereas for the first-order methods big values of CFL can be considered, the second order schemes present some oscillations related to the time integrator: a linear analysis performed by M. López-Fernández shows that the method is stable for CFL values lower than $1 + \sqrt{2}$. Moreover, the numerical solutions obtained with the piecewise constant reconstruction $\widetilde{Q}_i$ present more oscillations.

Furthermore, due to the well-balanced property of the methods, they are able to recover the stationary solution once the perturbation has left the domain. This is shown in Table 3, where L^1-errors between the stationary solution and the numerical solutions at time $t = 5$ have been computed for IEWBMi, $i = 1, 2$, using a 400-cell mesh and CFL$= 2$.

5.2. Burgers equation

Let us consider now the Burgers equation with a nonlinear source term

$$u_t + \left(\frac{1}{2}u^2\right)_x = \alpha u^2, \tag{30}$$

where $\alpha \in \mathbb{R}$. Again, the stationary solutions can be easily obtained:

$$u^e(x) = Ce^{\alpha x}$$

Then, given a family of cell values $\{u_i^n\}$, the stationary solution $u_i^{e,n}(x)$ sought in the first step of the reconstruction procedure is

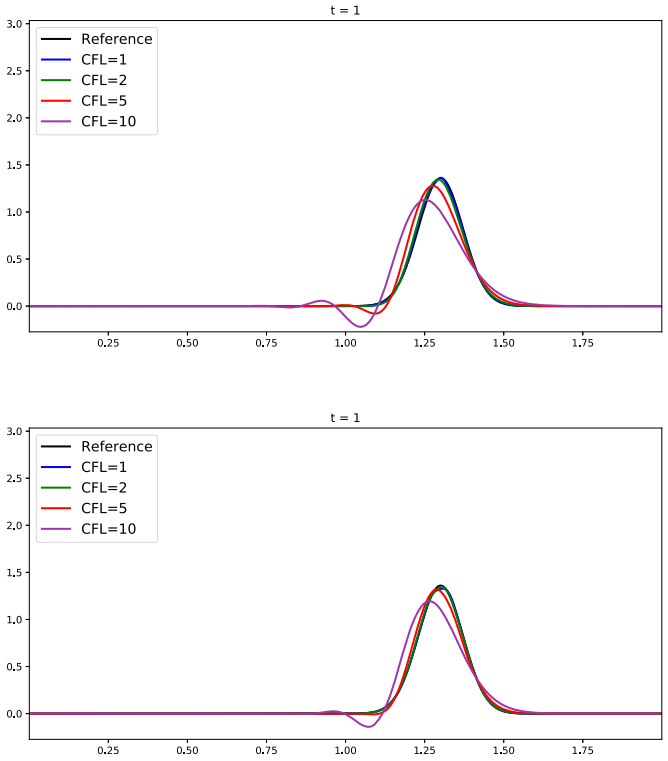

Fig. 2. Transport equation: Test 2. Differences between e^x and the numerical solutions obtained with IEWBM2 for different CFL values at $t = 1$. Top: PWCR. Bottom: PWLR.

$$u_i^{e,n}(x) = u_i^n e^{\alpha(x-x_i)}.$$

Exactly well-balanced methods are considered again.

Due to the non-linearity of the flux and the source term, nonlinear systems have to be solved now to find the time fluctuations. A numerical method for nonlinear systems of algebraic equations is required. In particular, in this problem the Newton's method is considered. For the first-order methods, only one iteration of the Newton's method is performed. The Rusanov numerical flux

$$\mathbb{F}(u, v) = \frac{c}{2}(f(u) + f(v)) - \frac{k}{2}(v - u),$$

is considered again, where k is the viscosity constant.

5.2.1. Test 1: stationary solution

We consider the space interval $[0, 2]$, the time interval $[0, 1000]$, $\alpha = 1$, and CFL=2. As initial condition, we consider the stationary solution

$$u_0(x) = e^x.$$

L^1 errors between the initial and final cell-averages have been computed for IEWBMp, $p = 1, 2$, using a 200-cell mesh for different times (see Table 4).

5.2.2. Test 2: perturbation of a stationary solution

We consider now the initial condition:

$$u_0(x) = e^x + 0.4e^{-25(x-0.4)^2}.$$

A reference solution has been computed using again IEWBM2 with piecewise linear reconstruction $\widetilde{Q}_i$ with a 3200-cell mesh. The numerical solutions obtained using different values of the CFL number are shown in Figs. 3-4. Notice that, unlike the linear case, no oscillations appear for second-order methods for large CFL values. Moreover, similar results are obtained with the piecewise constant and linear reconstructions $\widetilde{Q}_i$.

Table 5 shows the L^1-differences between the underlying stationary solution and the numerical solutions obtained with IEWBMp, $p = 1, 2$ at time $t = 10$ (once the perturbation has left the computational domain) using a 400-cell mesh and CFL$= 2$. Again, the stationary solution is recovered to machine precision.

Table 4
Burgers equation: Test 1. L^1-errors between the stationary and the numerical solution at $t = 1, 10, 100, 1000$ for IEWBM1 and IEWBM2 with piecewise constant (PWCR) or piecewise linear (PWLR) reconstruction $\widetilde{Q}_i$.

t	IEWBM1	IEWBM2	
		PWCR	PWLR
1	1.54e-13	1.32e-13	1.56e-13
10	1.54e-13	1.31e-13	1.56e-13
100	1.54e-13	1.31e-13	1.565e-13
1000	1.54e-13	1.31e-13	1.56e-13

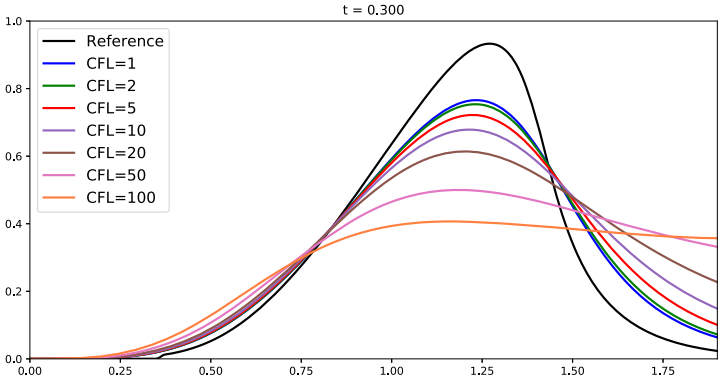

Fig. 3. Burgers equation: Test 2. Differences between e^x and the numerical solutions obtained with IEWBM1 using different CFL values at $t = 0.3$.

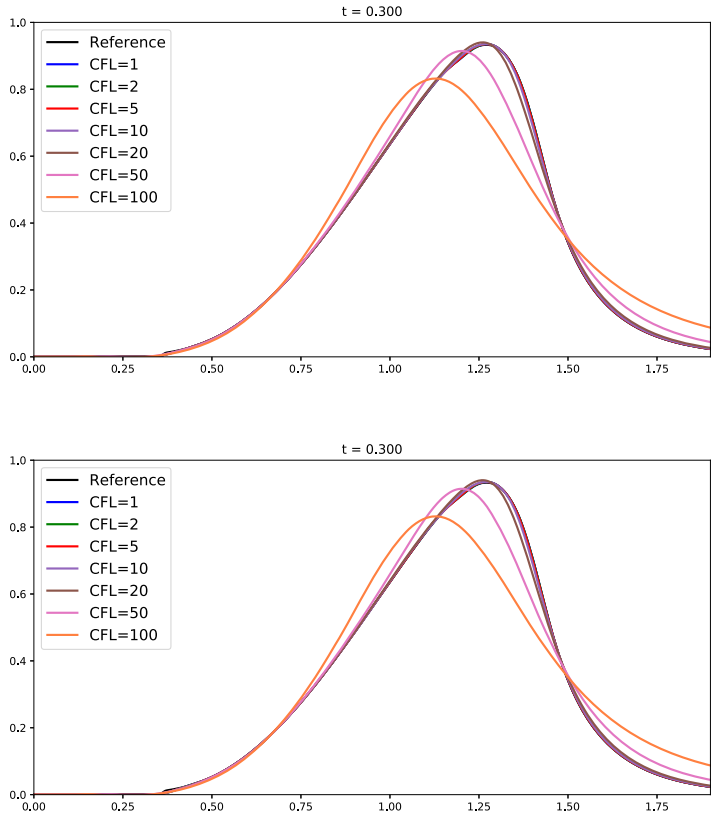

Fig. 4. Burgers equation: Test 2. Differences between e^x and the numerical solutions obtained with IEWBM2 using different CFL values at $t = 0.3$. Top: PWCR. Bottom: PWLR.

Table 5
Burgers equation: Test 2. Differences in L^1-norm between the stationary and the numerical solution at $t = 10$ for IEWBM1 and IEWBM2 with piecewise constant (PWCR) or piecewise linear (PWLR) reconstruction $\widetilde{Q}_i$.

IEWBM1	IEWBM2	
	PWCR	PWLR
1.54e-13	1.32e-13	1.56e-13

Table 6
Burgers equation: Test 3. Differences in L^1-norm between the reference and the numerical solutions at $t = 0.5$ for IEWBM1 and IEWBM2 with piecewise constant (PWCR) or piecewise linear (PWLR) reconstruction $\widetilde{Q}_i$.

Cells	IEWBM1		IEWBM2			
			PWCR		PWLR	
	Error	Order	Error	Order	Error	Order
25	1.67e-02	-	1.81e-03	-	1.81e-03	-
50	7.42e-02	1.17	4.76e-04	1.93	4.76e-04	1.93
100	4.79e-03	0.63	1.06e-04	2.16	1.06e-04	2.16
200	2.74e-02	0.81	2.99e-05	1.83	2.99e-05	1.83
400	1.48e-03	0.89	8.00e-06	1.90	8.00e-03	1.90
800	7.69e-04	0.95	2.02e-06	1.99	2.02e-06	1.99
1600	3.93e-04	0.97	4.85e-07	2.00	4.85e-07	2.06

5.2.3. Test 3: order test

We consider now the initial condition:

$$u_0(x) = 0.1e^x + 0.5e^{-25(x-1.0)^2}.$$

A reference solution has been computed with IEWBM2 and the piecewise linear reconstruction using a 6400-cell mesh. Table 6 shows the errors in L^1-norm with respect to the reference solution for EWBM1 and EWBM2 for both the piecewise constant and linear reconstructions: as it can be checked, the errors decrease with the number of cells at the expected convergence rate.

5.3. Shallow water equations

Let us consider now the 1d shallow water system with Manning friction

$$U_t + f(U)_x = S_1(U)H_x + S_2(U),$$

where

$$U = \begin{pmatrix} h \\ q \end{pmatrix}, \quad f(U) = \begin{pmatrix} q \\ \frac{q^2}{h} + \frac{g}{2}h^2 \end{pmatrix}, \quad S_1(U) = \begin{pmatrix} 0 \\ gh \end{pmatrix}, \quad S_2(U) = \begin{pmatrix} 0 \\ -\frac{kq|q|}{h^\mu} \end{pmatrix}.$$

The variable x makes reference to the axis of the channel and t is the time; $q(x,t)$ and $h(x,t)$ are the discharge and the thickness, respectively; $g = 9.81$ is the gravity; $H(x)$ is the depth function measured from a fixed reference level; k is the Manning friction coefficient and μ is set to $\frac{7}{3}$.

The eigenvalues of the system are

$$\lambda^{\pm} = u \pm c,$$

with $c = \sqrt{gh}$. The flow regime is characterized by the Froude number:

$$Fr(U) = \frac{|u|}{c}. \tag{31}$$

The flow is subcritical if $Fr < 1$, critical if $Fr = 1$ or supercritical if $Fr > 1$.

The stationary solutions satisfy the ODE system

$$\begin{cases} \left(-u^2 + gh\right) h_x = ghH_x - \dfrac{kq|q|}{h^\mu}, \\ q_x = 0. \end{cases} \tag{32}$$

Since the explicit expression of the stationary solutions is not available, well-balanced methods will be designed in which RK-collocation methods are used to approximate them. Different schemes are considered:

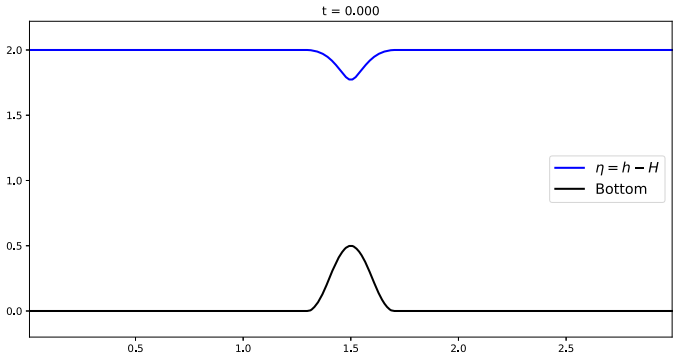

Fig. 5. Shallow water equations without friction: Test 1. Initial condition: subcritical stationary solution.

- Fully implicit schemes, where the flux and the source term are treated implicitly.
- Semi-implicit schemes for problems without friction, in which the advection term $\left(\frac{q^2}{h}\right)$ is treated explicitly and the equation of h, the pressure term $\left(\frac{1}{2}gh^2\right)$ and the source term are treated implicitly.
- Semi-implicit schemes for problems with friction, in which only the source term $\left(-\frac{kq|q|}{h^\mu}\right)$ is treated implicitly.

While the implementation of the two first types of methods above leads to solve coupled nonlinear algebraic systems at every stage of the RK solvers, in the third case of semi-implicit schemes for problems with friction, in which only the friction term is implicitly treated, local nonlinear equations have to be solved at every cell. Fixed-point iterations are considered in all cases.

5.3.1. Test 1: stationary solution

Let us first check the well-balanced property of the methods for the model without friction ($k = 0$). We consider $x \in [0, 3]$, $t \in [0, 1000]$ and CFL$= 2.0$. As initial condition, we consider the subcritical stationary solution which solves the Cauchy problem:

$$\begin{cases} q_x = 0, \\ (-u^2 + gh)h_x = ghH_x, \\ h(0) = 2.0 + H(0),\ q(0) = 3.5, \end{cases}$$

where the depth function is given by

$$H(x) = \begin{cases} -0.25(1 + \cos(5\pi(x + 0.5))) & \text{if} \quad 1.3 \le x \le 1.7, \\ 0 & \text{otherwise}, \end{cases} \tag{33}$$

(see Fig. 5). Table 7 shows the L^1 errors between the initial and final cell-averages, at various times, for IWBMp, SIWBMp, $p = 1, 2$, using a 200-cell mesh.

5.3.2. Test 2: order test

We now simulate a perturbation of a non-stationary smooth solution for the model without friction ($k = 0$). In particular, we consider $x \in [-5, 5]$, $t \in [0, 0.5]$, CFL$= 2.0$, and the depth function:

$$H(x) = 1.0 - 0.5e^{-x^2}. \tag{34}$$

The initial condition is given by:

$$q_0(x) = 0, \quad h_0(x) = 0.1e^{-5.0x^2},$$

(see Fig. 6). A 200-cell mesh is considered and a reference solution with a 1600-cell mesh using IWBM2 with the piecewise linear reconstruction has been obtained. The different implicit and semi-implicit methods have been compared (see Fig. 7). As expected, the numerical solutions obtained with first-order schemes are more diffusive than those given by second-order methods. Moreover, semi-implicit methods give better results than fully implicit schemes in the first-order case. Concerning the second-order schemes, the piecewise constant and linear reconstructions give similar results. No spurious oscillations appear for CFL$= 2$.

Table 7
Shallow water equations without friction: Test 1. Differences in L^1-norm between the stationary and the numerical solution at $t = 1, 10, 100, 1000$ for IWBM1, SIWBM1, IWBM2 and SIWBM2 with piecewise constant (PWCR) or piecewise linear (PWLR) reconstruction $\widetilde{Q}_i$ for a 200-cell mesh.

Implicit methods						
t	IWBM1		IWBM2			
			PWCR		PWLR	
	h	q	h	q	h	q
1	5.33e-15	4.88e-15	3.55e-15	7.55e-15	3.55e-15	6.22e-15
10	4.00e-15	3.11e-15	1.04e-14	2.13e-14	1.26e-14	4.46e-14
100	4.00e-15	3.11e-15	1.04e-14	2.13e-14	1.26e-14	4.45e-14
1000	4.00e-15	3.11e-15	1.04e-14	2.13e-14	1.25e-14	4.45e-14
Semi-implicit methods						
t	IWBM1		IWBM2			
			PWCR		PWLR	
	h	q	h	q	h	q
1	2.00e-15	7.11e-15	5.11e-15	8.00e-15	5.55e-15	8.44e-15
10	3.03e-15	2.22e-14	7.02e-15	9.49e-15	4.27e-14	2.49e-14
100	3.03e-15	2.22e-14	7.02e-15	9.49e-15	4.27e-14	2.49e-14
1000	3.03e-15	2.22e-14	7.02e-15	9.49e-15	4.27e-14	2.49e-14

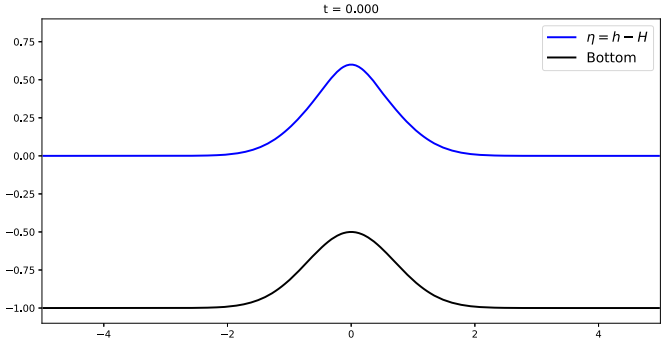

Fig. 6. Shallow water equations without friction: Test 2. Initial condition.

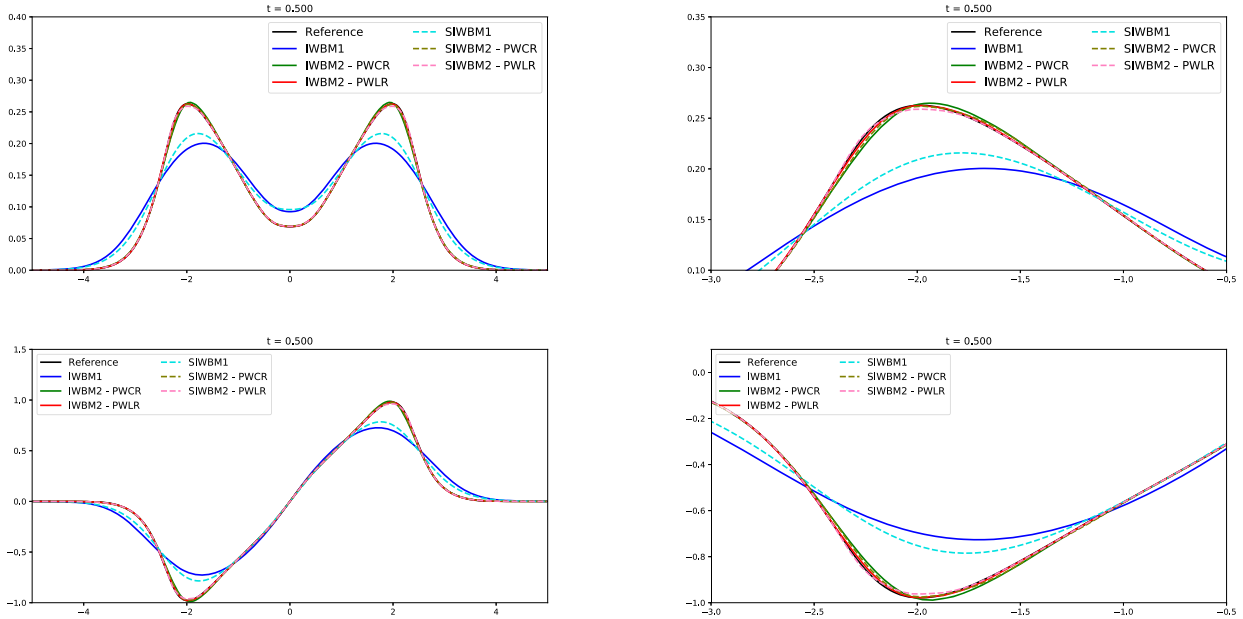

Fig. 7. Shallow water equations without friction: Test 2. Numerical solutions for IWBMp, SIWBMp, $p = 1, 2$ with CFL$= 2$ at $t = 0.5$. Top: η. Bottom: q.

Table 8
Shallow water equations without friction: Test 2. Differences in L^1-norm with respect to the reference solution and convergence rates for h at $t = 0.5$ for IWBM1 and IWBM2 with piecewise constant (PWCR) or picewise linear (PWLR) reconstruction $\widetilde{Q}_i$ for the thickness h.

Cells	IWBM1		IWBM2			
			PWCR		PWLR	
	Error	Order	Error	Order	Error	Order
25	2.60e-01	-	2.90e-01	-	1.57e-01	-
50	2.32e-01	0.16	1.31e-01	1.14	4.91e-02	1.68
100	2.06e-01	0.17	4.90e-02	1.42	1.37e-02	1.84
200	9.88e-01	1.06	1.42e-01	1.78	3.52e-03	1.96
400	4.20e-02	1.23	3.73e-03	1.94	8.48e-04	2.05

Table 9
Shallow water equations without friction: Test 2. Differences in L^1-norm with respect to the reference solution and convergence rates for h at $t = 0.5$ for IWBM1 and IWBM2 with piecewise constant (PWCR) or picewise linear (PWLR) reconstruction $\widetilde{Q}_i$ for the discharge q.

Cells	IWBM1		IWBM2			
			PWCR		PWLR	
	Error	Order	Error	Order	Error	Order
25	1.35	-	1.17	-	5.55e-01	-
50	1.04	0.37	5.62e-01	1.05	2.04e-01	1.45
100	7.38-01	0.40	1.92e-01	1.55	5.56e-02	1.87
200	3.98e-01	0.89	5.72e-02	1.74	1.44e-02	1.95
400	1.95e-01	1.03	1.51e-02	1.92	3.48e-03	2.05

Table 10
Shallow water equations without friction: Test 2. Differences in L^1-norm with respect to the reference solution and convergence rates for h at $t = 0.5$ for SIWBM1 and SIWBM2 with piecewise constant (PWCR) or picewise linear (PWLR) reconstruction $\widetilde{Q}_i$ for the thickness h.

Cells	SIWBM1		SIWBM2			
			PWCR		PWLR	
	Error	Order	Error	Order	Error	Order
25	4.82e-01	-	1.41e-01	-	1.14e-01	-
50	3.70e-01	0.38	5.34e-02	1.40	2.86e-02	1.99
100	2.24e-01	0.72	1.72e-02	1.63	6.33e-03	2.18
200	1.39e-01	0.68	4.55e-03	1.92	1.53e-03	2.05
400	7.38e-02	0.92	1.16e-03	1.97	3.62e-04	2.08

Table 11
Shallow water equations without friction: Test 2. Differences in L^1-norm with respect to the reference solution and convergence rates for h at $t = 0.5$ for IWBM1 and IWBM2 with piecewise constant (PWCR) or picewise linear (PWLR) reconstruction $\widetilde{Q}_i$ for the discharge q.

Cells	SIWBM1		SIWBM2			
			PWCR		PWLR	
	Error	Order	Error	Order	Error	Order
25	1.74	-	6.10e-01	-	3.33e-01	-
50	1.47	0.24	2.23e-01	1.45	9.40e-02	1.83
100	9.83e-01	0.74	6.88e-02	1.69	2.25e-02	2.06
200	5.83e-01	0.60	1.84e-02	1.91	5.64e-03	2.00
400	3.01e-01	0.95	4.69e-02	1.97	1.35e-03	2.07

Tables 8–11 show the order for the implicit and semi-implicit methods. The expected convergence rates have been obtained for both variables h and q.

As expected, second-order schemes which make use of piecewise linear reconstruction for $\widetilde{Q}_i$ are systematically more accurate than the ones based on piecewise constant reconstruction, even if the order of accuracy is the same. It is interesting to observe that semi-implicit schemes are more accurate than fully implicit schemes and even of explicit schemes. This makes semi-implicit schemes the most cost-effective since they are more accurate and less expensive than fully implicit schemes, and they allow larger CFL numbers and are even more accurate than explicit schemes. Fully implicit schemes are more dissipative than semi-implicit schemes, which explains the higher accurate for the same grid and CFL number. Furthermore, for low Froude number flow, they are also less dissipative than explicit schemes. The reason is that explicit schemes have to use a larger numerical viscosity than semi-implicit ones in the Rusanov numerical flux function. This

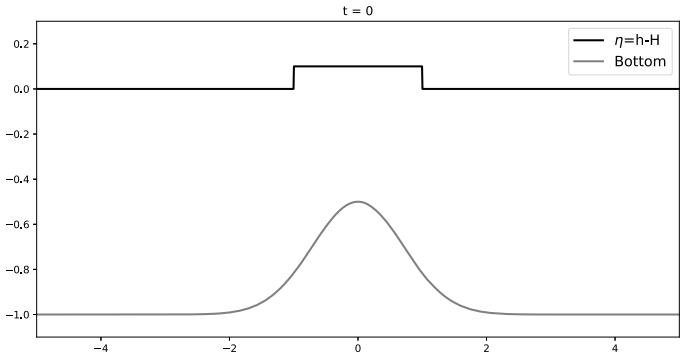

Fig. 8. Shallow water equations without friction: Test 3. Initial condition.

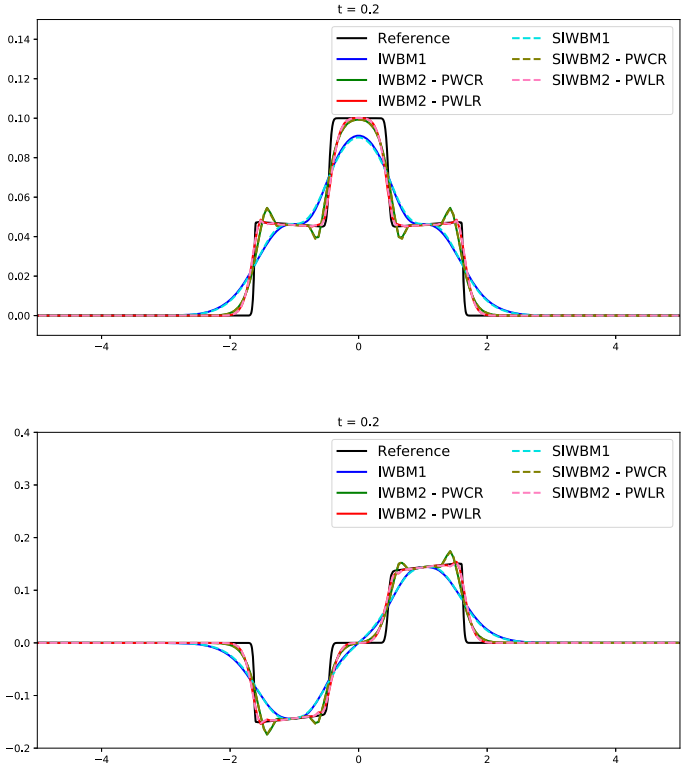

Fig. 9. Shallow water equations without friction: Test 3. Numerical solutions for IWBMp, SIWBMp, $p = 1, 2$ with CFL$= 2$ at $t = 0.2$. Top: η. Bottom: q.

effect is well known and discussed in the detail in the literature for numerical methods for all Mach-number flows (see for example [39] for the analysis of the phenomenon, [16,2,4] for second order accurate finite volume schemes to treat all Mach number flows in compressible Euler equations, [13] for high order schemes, and [73] for applications in astrophysics).

5.3.3. Test 3: shock waves

We consider again the model without friction ($k = 0$) with a discontinuous initial condition that generates two shock waves traveling in oposite directions. We consider the space interval $[-5, 5]$ and the time interval $[0, 0.5]$ and CFL=2. The depth function is again given by (34). As initial condition, we consider the functions:

$$q_0(x) = 0, \quad h_0(x) = \begin{cases} H(x) & \text{if } |x| \geq 1; \\ H(x) + 0.1 & \text{if } |x| < 1; \end{cases}$$

(see Fig. 8).

A reference solution with a 1600-cell mesh using the SIWBM2 with piecewise linear reconstruction for $\widetilde{Q}_i$ has been obtained. Figs. 9-10 show the numerical solutions obtained with the different methods at times $t = 0.2, 0.5$.

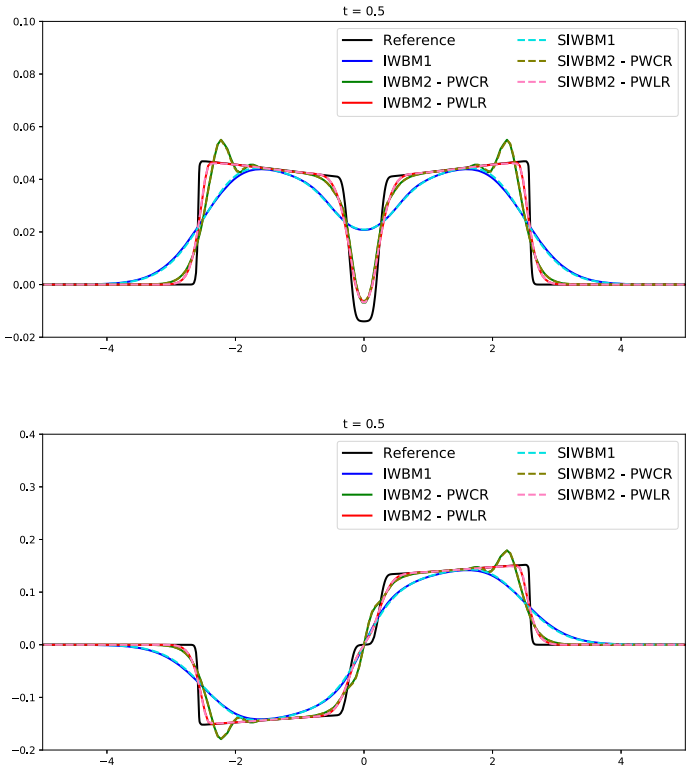

Fig. 10. Shallow water equations without friction: Test 3. Numerical solutions for IWBMp, SIWBMp, $p = 1, 2$ with CFL$= 2$ at $t = 0.5$. Top: η. Bottom: q.

Observe that when using a piecewise constant reconstruction $\widetilde{Q}_i(x)$, the numerical solution is less accurate and more oscillatory.

5.3.4. Test 4: convergence to a steady state

The goal now is to compare the ability of explicit and implicit schemes to reach a stationary solution as time increases. We consider again the model without friction ($k = 0$). Only the first-order methods EXWBM1 and IWBM1 are considered here.

The space interval is $[0, 3]$ and the depth function is given again by (33). The initial condition is $h(x, 0) = 2.0$ and $q(x, 0) = 0.0$. The boundary conditions are the following

$$q(0, t) = 1.0, \quad h(3, t) = 2.0.$$

A 100-cell mesh is considered. The numerical solution is run until a stationary state is reached: the numerical method is stopped if

$$\frac{\max_i |U_i^{n+1} - U_i^n|}{\Delta t} < \varepsilon, \tag{35}$$

where ε is a fixed threshold. In this test, we take $\varepsilon =$1e-12. Fig. 11 shows the stationary solution and Table 12 shows, for every numerical method, the time in seconds needed to reach a steady state, the difference in L^1-norm between the reached steady state and the subcritical stationary solution that solves the problem

$$\begin{cases} q_x = 0, \\ (-u^2 + gh)h_x = ghH_x, \\ h(3) = 2.0,\ q(0) = 1.0, \end{cases} \tag{36}$$

the CPU times (in seconds), the total number of iterations in time associated to the time step Δt and the total and maximum (per time step) number of iterations of the fixed-point algorithm applied to solve the nonlinear problems are in the case of fully implicit schemes. As expected, the implicit methods converge faster to the stationary solution. Notice that if the problem is just to capture the global stationary solution, then first order schemes may be perfectly adequate. However the interplay between time accuracy and the final stationary solution (in case the latter depends on the initial conditions as well and not only on the boundary conditions) is not obvious and it will be explored in future work.

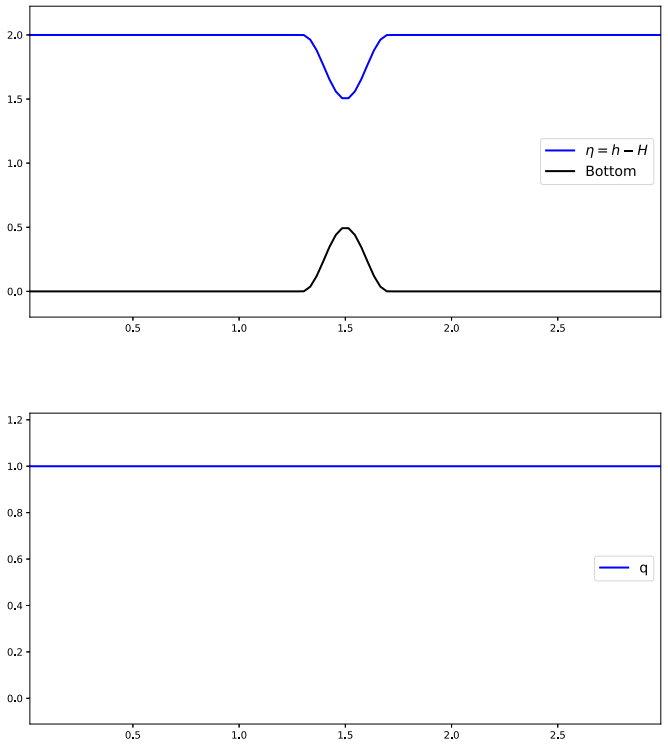

Fig. 11. Shallow water equations without friction: Test 4. Stationary solution.

Table 12
Shallow water equations without friction: Test 4. Time needed to reach a steady state, differences in L^1-norm between the reached steady state and the subcritical stationary solution which solves the problem (36), CPU times, total number of iterations in time associated to the time step Δt and total and maximum number of iterations per time step of the fixed-point algorithm applied to solve the nonlinear problems are in the case of fully implicit schemes.

EXWBM1							
CFL	Times of convergence	Errors of convergence		CPU times	Iterations in time	Fixed-point iterations	
		h	q			Total	Max
0.5	177.91	2.55e-14	1.61e-13	80.90	52465	-	-
0.99	159.34	1.35e-13	1.29e-12	49.35	29586	-	-
IWBM1							
CFL	Times of convergence	Errors of convergence		CPU times	Iterations in time	Fixed-point iterations	
		h	q			Total	Max
2	129.51	1.96e-13	1.65e-12	186.96	10660	97720	26
10	85.84	2.17e-13	1.83e-12	38.40	1413	36265	87
20	64.04	1.55e-13	1.17e-12	21.57	527	22606	201
50	41.64	4.42e-14	1.62e-12	20.60	138	26194	254

Notice that, for CFL=50, in spite of the fact that the total number of iterations of the fixed-point algorithm is bigger than in the case of CFL=20, less computational effort is required since the total number of well-balanced reconstructions is smaller.

5.3.5. Test 5: stationary solution for the model with friction

Let us check the well-balanced property of the methods for the model with friction. In this test, the Manning friction is $k = 0.01$ and the space interval is $[0, 1]$. The depth function is given by

$$H(x) = 1 - \frac{1}{2} - \frac{e^{\cos(4\pi x)} - e^{-1}}{e - e^{-1}}. \tag{37}$$

We consider a supercritical stationary solution: the solution of (32) with initial conditions $q(0) = 3$ and $h(0) = 0.3$ (see Fig. 12), obtained numerically by solving system (32) using the mid-point rule (see [50]). We consider a 100-cell mesh and

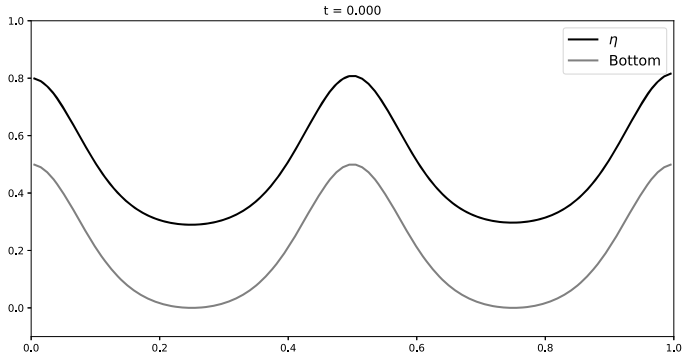

Fig. 12. Shallow water equations with friction: Test 5. Initial condition: supercritical stationary solution. Free surface and bottom.

Table 13
Shallow water equations with friction: Test 5. Differences in L^1-norm between the stationary and the numerical solution at $t = 1, 10, 100, 1000$ for IWBM1, SIWBM1, IWBM2 and SIWBM2 with piecewise constant (PWCR) or piecewise linear (PWLR) reconstruction $\widetilde{Q}_i$ for a 100-cell mesh.

Implicit methods						
t	IWBM1		IWBM2			
			PWCR		PWLR	
	h	q	h	q	h	q
1	6.11e-16	8.88e-16	9.44e-16	9.36e-15	6.66e-16	6.22e-15
10	4.27e-16	4.87e-16	9.44e-16	9.03e-15	8.97e-16	9.21e-15
100	4.27e-16	4.87e-16	9.44e-16	9.03e-15	8.97e-16	9.21e-15
1000	4.27e-16	4.87e-16	9.44e-16	9.03e-15	8.97e-16	9.21e-15
Semi-implicit methods						
t	IWBM1		IWBM2			
			PWCR		PWLR	
	h	q	h	q	h	q
1	7.21e-16	6.66e-15	9.44e-16	9.76e-15	8.33e-16	6.21e-15
10	7.21e-16	6.66e-15	3.89e-16	1.33e-15	8.33e-16	8.44e-15
100	7.21e-16	6.66e-15	3.89e-16	1.33e-15	8.33e-16	8.44e-15
1000	7.21e-16	6.66e-15	3.89e-16	1.33e-15	8.33e-16	8.44e-15

the final time is $t = 1000$. Notice that, at variance with the low Froude number stationary solutions, in the supercritical case the profile of the free surface is almost parallel to the bottom profile, so that $h(x)$ is almost constant. Table 13 shows the L^1-errors between the initial and the approximated cell-averages at times $t = 1, 10, 100, 1000$ given by SIWBM1, IWBM1, SIWBM2 and IWBM2 with piecewise constant (PWCR) or piecewise linear (PWLR) reconstruction $\widetilde{Q}_i$.

5.3.6. Test 6: perturbation of a stationary solution for the model with friction

In this test, the Manning friction is again $k = 0.01$. The depth function is given by (37). We consider a perturbation of the supercritical stationary solution: the initial condition $U_0(x) = [h_0(x), q_0(x)]^T$ given by

$$h_0(x) = \begin{cases} h^*(x) + 0.05, & \text{if } x \in \left[\frac{2}{7}, \frac{3}{7}\right] \cup \left[\frac{4}{7}, \frac{5}{7}\right], \\ h^*(x), & \text{otherwise,} \end{cases}$$

$$q_0(x) = \begin{cases} q^*(x) + 0.5, & \text{if } x \in \left[\frac{2}{7}, \frac{3}{7}\right] \cup \left[\frac{4}{7}, \frac{5}{7}\right], \\ q^*(x), & \text{otherwise,} \end{cases}$$

where $U^*(x) = [h^*(x), q^*(x)]^T$ is the stationary solution considered in Test 5 (see Fig. 13). We consider a 100-cell mesh and the numerical simulation is run until $t = 2$. A reference solution computed with a 800-cell mesh using SIWBM2 with piecewise constant reconstruction $\widetilde{Q}_i$ has been considered. Figs. 14-15 show the evolution of the perturbation at times $t = 0.01$ and $t = 0.05$ for SIWBM1 and SIWBM2 with piecewise constant (PWCR) or piecewise linear (PWLR) reconstruction $\widetilde{Q}_i$ and Table 14 shows the differences in L^1-norm between the stationary and the numerical solutions at $t = 2$. As expected, the stationary solution is recovered with machine precision.

Fully implicit schemes have been also considered with CFL=2, recovering with machine precision the supercritical stationary solution at the final time $t = 2s$ (see Table 15, where the errors L^1-norm between the stationary and the numerical

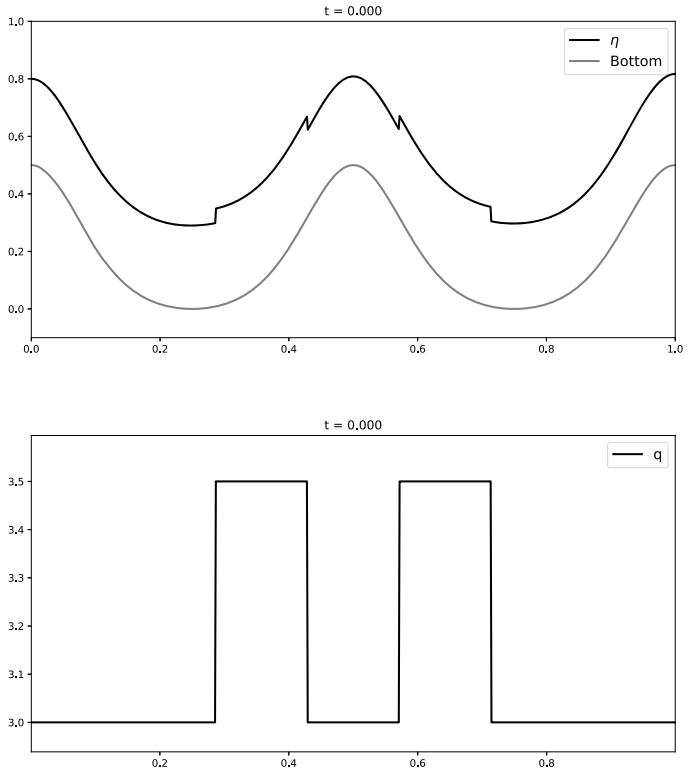

Fig. 13. Shallow water equations with friction: Test 6. Initial condition: perturbation of a supercritical stationary solution. Top: η. Bottom: q.

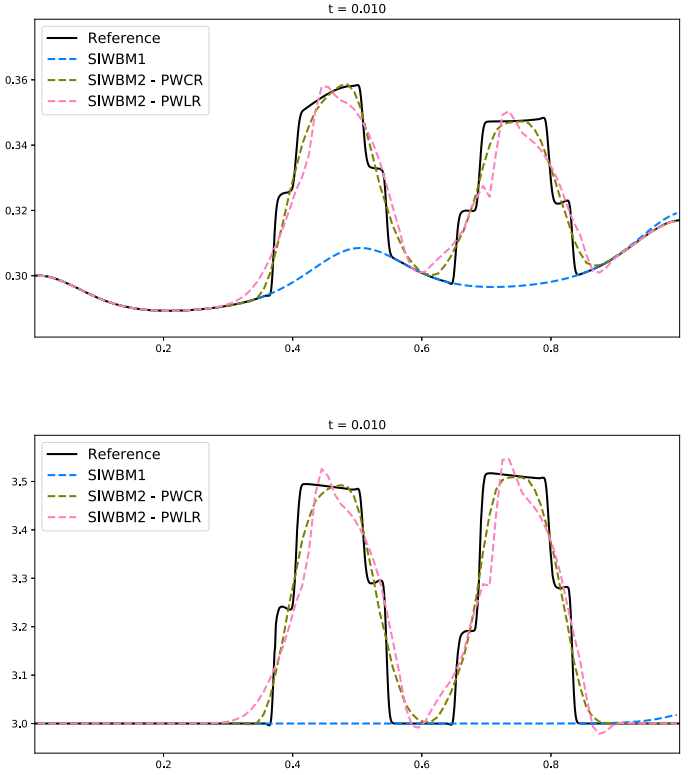

Fig. 14. Shallow water equations with friction: Test 6. Numerical solutions for SIWBMp, $p = 1, 2$ with CFL$= 0.9$ at $t = 0.01$. Top: h. Bottom: q.

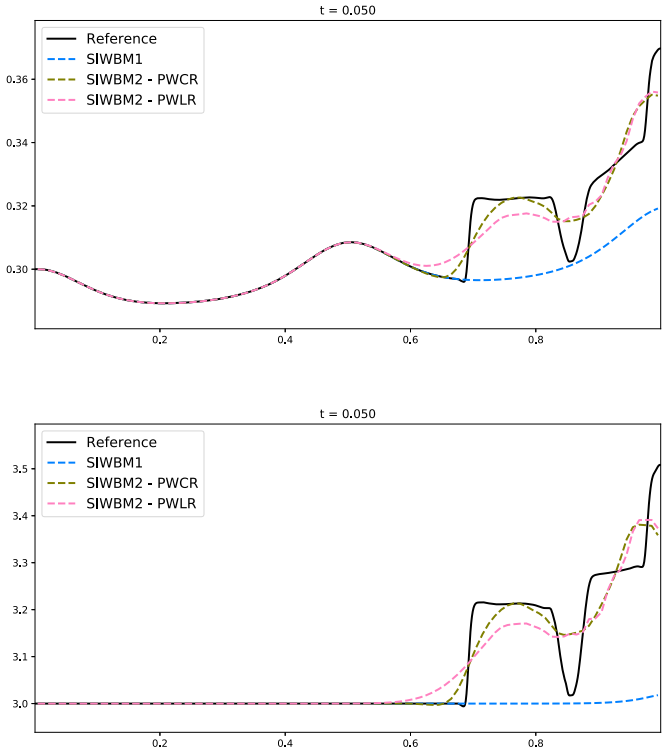

Fig. 15. Shallow water equations with friction: Test 6. Numerical solutions for SIWBMp, $p = 1, 2$ with CFL$= 0.9$ at $t = 0.05$. Top: h. Bottom: q.

Table 14
Shallow water equations with friction: Test 6. Differences in L^1-norm between the stationary and the numerical solution at $t = 2$ for SIWBM1 and SIWBM2 with piecewise constant (PWCR) or piecewise linear (PWLR) reconstruction $\widetilde{Q}_i$ for a 100-cell mesh.

Semi-implicit methods					
SIWBM1		SIWBM2			
		PWCR		PWLR	
h	q	h	q	h	q
9.99e-16	1.15e-14	4.44e-16	1.33e-15	6.10e-16	5.32e-15

Table 15
Shallow water equations with friction: Test 6. Differences in L^1-norm between the stationary and the numerical solution at $t = 2$ for IWBM1 and IWBM2 with piecewise constant (PWCR) or piecewise linear (PWLR) reconstruction $\widetilde{Q}_i$ for a 100-cell mesh.

Implicit methods					
IWBM1		IWBM2			
		PWCR		PWLR	
h	q	h	q	h	q
5.00e-16	4.41e-16	1.50e-15	1.51e-14	8.33e-16	7.55e-15

solutions at $t = 2$ for IWBM1 and IWBM2 with piecewise constant (PWCR) or piecewise linear (PWLR) reconstruction $\widetilde{Q}_i$ are shown).

6. Conclusions and forthcoming work

Following some previous work of the authors [24,28,48–50], we develop a general procedure to design high-order implicit and semi-implicit numerical schemes for any one-dimensional system of balance laws. Note that the main ingredient of these methods is a well-balanced reconstruction operator. A general result proving the well-balanced property of these numerical methods is stated. We checked the new formulation with several numerical tests, considering scalar problems such as the linear transport equation and the Burgers equation, and more complex systems such as shallow water in presence of variable bathymetry and Manning friction. Notice that, when both the flux and the source term of (1) are (equally) stiff, the system may relax to a stationary solution of the ODE system (2) in a very short time. If one is interested in effi-

ciently capturing the stationary solution, then it is advisable to adopt an implicit (or semi-implicit) scheme which is at the same time well-balanced. This is shown in a numerical test for the shallow water model.

Future work will include applications to more general systems whose source contains a stiff relaxation and a non-stiff term, i.e. systems of the form

$$u_t + f(u)_x = \frac{1}{\epsilon} S(u) + G(u, x), \tag{38}$$

that in the limit of vanishing ϵ relaxes to a lower dimensional system of balance laws of the form

$$v_t + \boldsymbol{f}(v)_x = \boldsymbol{g}(v, x), \tag{39}$$

where $v(x,t) = Q\,u(x,t) \in \mathbb{R}^n$, $n < N$, $Q \in \mathbb{R}^{n\times N}$, $Q\,S(u) = 0$, and $\boldsymbol{f} = Q\,f(E(v))$, with $u = E(v)$, $\boldsymbol{g}(u,x) = Q\,G(E(u),x)$. In such cases the limit equation admits non-trivial stationary solutions which must be accurately approximated. Our aim will be to design numerical schemes for systems (38) which become consistent and well-balanced schemes for systems (39) as the relaxation parameter vanishes, which are said to be *Asymptotic Preserving and Well-Balanced (APWB)* (see [62,61,34,78]). A natural framework to define such numerical schemes is the combination of well-balanced finite-volume schemes and IMEX methods.

A second important extension concerns the application of this framework to problems in more space dimensions, with the specific goal to capture non trivial stationary solutions of systems of balance laws, along the lines of the pioneering work of Moretti and Abbett [74], who captured the stationary flow around a blunt body by looking for the stationary solutions of a time dependent problem.

Acknowledgements

We would like to thank M. López-Fernández for the linear stability analysis performed in Test 2 for the transport equation. This work is partially supported by projects RTI2018-096064-B-C21 funded by MCIN/AEI/10.13039/501100011033 and "ERDF A way of making Europe", projects P18-RT-3163 of Junta de Andalucía and UMA18-FEDERJA-161 of Junta de Andalucía-FEDER-University of Málaga. G. Russo and S. Boscarino acknowledge partial support from the Italian Ministry of University and Research (MIUR), PRIN Project 2017 (No. 2017KKJP4X) entitled "Innovative numerical methods for evolutionary partial differential equations and applications". I. Gómez-Bueno is also supported by a Grant from "El Ministerio de Ciencia, Innovación y Universidades", Spain (FPU2019/01541) funded by MCIN/AEI/10.13039/501100011033 and "ESF Investing in your future". Funding for open access charge: Universidad de Málaga/CBUA.

References

[1] R. Abgrall, D. Santis, M. Ricchiuto, High-order preserving residual distribution schemes for advection-diffusion scalar problems on arbitrary grids, SIAM J. Sci. Comput. 36 (3) (January 2014) A955–A983.
[2] Koottungal Revi Arun, Sebastian Noelle, Maria Lukacova-Medvidova, Claus-Dieter Munz, an asymptotic preserving all Mach number scheme for the Euler equations of gas dynamics, preprint, October 2012.
[3] Emmanuel Audusse, François Bouchut, Marie-Odile Bristeau, Rupert Klein, Benoît Perthame, A fast and stable well-balanced scheme with hydrostatic reconstruction for shallow water flows, SIAM J. Sci. Comput. 25 (6) (2004) 2050–2065.
[4] Stavros Avgerinos, Florian Bernard, Angelo Iollo, Giovanni Russo, Linearly implicit all Mach number shock capturing schemes for the Euler equations, J. Comput. Phys. 393 (2019) 278–312.
[5] Jonas P. Berberich, Praveen Chandrashekar, Christian Klingenberg, High order well-balanced finite volume methods for multi-dimensional systems of hyperbolic balance laws, Comput. Fluids 219 (2021) 104858.
[6] Alfredo Bermudez, Elena Vazquez, Upwind methods for hyperbolic conservation laws with source terms, Comput. Fluids 23 (8) (1994) 1049–1071.
[7] Christophe Berthon, Christophe Chalons, A fully well-balanced, positive and entropy-satisfying Godunov-type method for the shallow-water equations, Math. Comput. 85 (299) (2016) 1281–1307.
[8] Christophe Berthon, Victor Michel-Dansac, A simple fully well-balanced and entropy preserving scheme for the shallow-water equations, Appl. Math. Lett. 86 (2018) 284–290.
[9] Luca Bonaventura, Enrique D. Fernández-Nieto, José Garres-Díaz, Gladys Narbona-Reina, Multilayer shallow water models with locally variable number of layers and semi-implicit time discretization, J. Comput. Phys. 364 (2018) 209–234.
[10] Sebastiano Boscarino, Philippe G. LeFloch, Giovanni Russo, High-order asymptotic-preserving methods for fully nonlinear relaxation problems, SIAM J. Sci. Comput. 36 (2) (2014) A377–A395.
[11] Sebastiano Boscarino, Lorenzo Pareschi, Giovanni Russo, Implicit-explicit Runge–Kutta schemes for hyperbolic systems and kinetic equations in the diffusion limit, SIAM J. Sci. Comput. 35 (1) (2013) A22–A51.
[12] Sebastiano Boscarino, Lorenzo Pareschi, Giovanni Russo, A unified IMEX Runge–Kutta approach for hyperbolic systems with multiscale relaxation, SIAM J. Numer. Anal. 55 (4) (2017) 2085–2109.
[13] Sebastiano Boscarino, Jingmei Qiu, Giovanni Russo, Tao Xiong, High order semi-implicit WENO schemes for all-Mach full Euler system of gas dynamics, SIAM J. Sci. Comput. 44 (2) (2022) B368–B394.
[14] Sebastiano Boscarino, Giovanni Russo, On a class of uniformly accurate IMEX Runge–Kutta schemes and applications to hyperbolic systems with relaxation, SIAM J. Sci. Comput. 31 (3) (2009) 1926–1945.
[15] Sebastiano Boscarino, Giovanni Russo, Flux-explicit IMEX Runge–Kutta schemes for hyperbolic to parabolic relaxation problems, SIAM J. Numer. Anal. 51 (1) (2013) 163–190.
[16] Sebastiano Boscarino, Giovanni Russo, Leonardo Scandurra, All Mach number second order semi-implicit scheme for the Euler equations of gas dynamics, J. Sci. Comput. 77 (2) (2018) 850–884.
[17] François Bouchut, Nonlinear Stability of Finite Volume Methods for Hyperbolic Conservation Laws: And Well-Balanced Schemes for Sources, Springer Science & Business Media, 2004.

[18] François Bouchut, Tomás Morales de Luna, A subsonic-well-balanced reconstruction scheme for shallow water flows, SIAM J. Numer. Anal. 48 (5) (2010) 1733–1758.
[19] Saray Busto Ulloa, M. Dumbser, A staggered semi-implicit hybrid finite volume / finite element scheme for the shallow water equations at all Froude numbers, Appl. Numer. Math. 175 (February 2022).
[20] Alberto Canestrelli, Michael Dumbser, Annunziato Siviglia, Eleuterio F. Toro, Well-balanced high-order centered schemes on unstructured meshes for shallow water equations with fixed and mobile bed, Adv. Water Resour. 33 (3) (2010) 291–303.
[21] Vicent Caselles, Rosa Donat, Gloria Haro, Flux-gradient and source-term balancing for certain high resolution shock-capturing schemes, Comput. Fluids 38 (1) (2009) 16–36.
[22] Manuel Castro, Tomás Chacón Rebollo, Enrique Fernández-Nieto, C. Parés, On well-balanced finite volume methods for nonconservative nonhomogeneous hyperbolic systems, SIAM J. Sci. Comput. 29 (January 2007) 1093–1126.
[23] Manuel Castro, José Gallardo, Carlos Parés, High order finite volume schemes based on reconstruction of states for solving hyperbolic systems with nonconservative products. Applications to shallow-water systems, Math. Comput. 75 (255) (2006) 1103–1134.
[24] Manuel Castro, José Gallardo, Juan López-García, Carlos Parés, Well-balanced high order extensions of Godunov's method for semilinear balance laws, SIAM J. Numer. Anal. 46 (January 2008) 1012–1039.
[25] Manuel J. Castro, Christophe Chalons, Tomás Morales de Luna, A fully well-balanced Lagrange-projection-type scheme for the shallow-water equations, SIAM J. Numer. Anal. 56 (5) (2018) 3071–3098.
[26] Manuel J. Castro, T. Morales de Luna, Carlos Parés, Well-Balanced Schemes and Path-Conservative Numerical Methods, vol. 18, Elsevier, 2017, pp. 131–175.
[27] Manuel J. Castro, Alberto Pardo Milanés, Carlos Parés, Well-balanced numerical schemes based on a generalized hydrostatic reconstruction technique, Math. Models Methods Appl. Sci. 17 (12) (2007) 2055.
[28] Manuel Jesús Castro, Carlos Parés, Well-balanced high-order finite volume methods for systems of balance laws, J. Sci. Comput. 82 (February 2020).
[29] Casulli Vincenzo, Semi-implicit finite difference methods for the two-dimensional shallow water equations, J. Comput. Phys. 86 (1) (1990) 56–74.
[30] Tomás Chacón Rebollo, Antonio Delgado, Enrique Fernández-Nieto, Asymptotically balanced schemes for non-homogeneous hyperbolic systems - application to the shallow water equations, C. R. Math. 338 (January 2004) 85–90.
[31] Tomás Chacón Rebollo, Antonio Delgado, Enrique Fernández-Nieto, A family of stable numerical solvers for the shallow water equations with source terms, Comput. Methods Appl. Mech. Eng. 192 (January 2003) 203–225.
[32] Christophe Chalons, Samuel Kokh, Maxime Stauffert, An All-Regime and Well-Balanced Lagrange-Projection Scheme for the Shallow Water Equations on Unstructured Meshes, Springer International Publishing, Cham, 2020, pp. 77–83.
[33] Praveen Chandrashekar, Markus Zenk, Well-balanced nodal discontinuous Galerkin method for Euler equations with gravity, J. Sci. Comput. 71 (2015) 11.
[34] Gui-Qiang Chen, C. David Levermore, Tai-Ping Liu, Hyperbolic conservation laws with stiff relaxation terms and entropy, Commun. Pure Appl. Math. 47 (6) (1994) 787–830.
[35] Yuanzhen Cheng, Alexander Kurganov, Moving-water equilibria preserving central-upwind schemes for the shallow water equations, Commun. Math. Sci. 14 (January 2016) 1643–1663.
[36] Alina Chertock, Shumo Cui, Alexander Kurganov, Seyma Nur Özcan, Eitan Tadmor, Well-balanced schemes for the Euler equations with gravitation: conservative formulation using global fluxes, J. Comput. Phys. 358 (2018) 36–52.
[37] Alina Chertock, Shumo Cui, Alexander Kurganov, Tong Wu, Well-balanced positivity preserving central-upwind scheme for the shallow water system with friction terms, Int. J. Numer. Methods Fluids 78 (April 2015).
[38] Alina Chertock, Michael Dudzinski, Alexander Kurganov, Maria Lukácová, Well-balanced schemes for the shallow water equations with Coriolis forces, Numer. Math. 138 (2018) 939–973.
[39] Stéphane Dellacherie, Analysis of Godunov type schemes applied to the compressible Euler system at low Mach number, J. Comput. Phys. 229 (4) (2010) 978–1016.
[40] Vivien Desveaux, Markus Zenk, Christophe Berthon, Christian Klingenberg, Well-balanced schemes to capture non-explicit steady states. RIPA model, Math. Comput. 85 (October 2015) 1.
[41] Vivien Desveaux, Markus Zenk, Christophe Berthon, Christian Klingenberg, A well-balanced scheme to capture non-explicit steady states in the Euler equations with gravity, Int. J. Numer. Methods Fluids 81 (2) (2016) 104–127.
[42] Michael Dumbser, Vincenzo Casulli, A staggered semi-implicit spectral discontinuous Galerkin scheme for the shallow water equations, Appl. Math. Comput. 219 (15) (2013) 8057–8077.
[43] Emmanuel Franck, Laura S. Mendoza, Finite volume scheme with local high order discretization of the hydrostatic equilibrium for the Euler equations with external forces, J. Sci. Comput. 69 (1) (2016) 314–354.
[44] Emmanuel Franck, Laurent Navoret, Semi-implicit two-speed well-balanced relaxation scheme for Ripa model, in: Robert Klöfkorn, Eirik Keilegavlen, Florin A. Radu, Jürgen Fuhrmann (Eds.), Finite Volumes for Complex Applications IX - Methods, Theoretical Aspects, Examples, Springer International Publishing, Cham, 2020, pp. 735–743.
[45] Gérard Gallice, Solveurs simples positifs et entropiques pour les systèmes hyperboliques avec terme source, C. R. Math. 334 (8) (2002) 713–716.
[46] P. Garcia-Navarro, M.E. Vazquez-Cendon, On numerical treatment of the source terms in the shallow water equations, Comput. Fluids 29 (8) (August 2000) 951–979.
[47] F.X. Giraldo, M. Restelli, High-order semi-implicit time-integrators for a triangular discontinuous Galerkin oceanic shallow water model, Int. J. Numer. Methods Fluids 63 (9) (2010) 1077–1102.
[48] Irene Gómez-Bueno, Manuel J. Castro, Carlos Parés, High-order well-balanced methods for systems of balance laws: a control-based approach, Appl. Math. Comput. 394 (2021) 125820.
[49] Irene Gómez-Bueno, Manuel Jesús Castro, Carlos Parés, Well-balanced reconstruction operator for systems of balance laws: numerical implementation, in: Recent Advances in Numerical Methods for Hyperbolic PDE Systems, Springer, 2021, pp. 57–77.
[50] Irene Gómez-Bueno, Manuel Jesús Castro Díaz, Carlos Parés, Giovanni Russo, Collocation methods for high-order well-balanced methods for systems of balance laws, Mathematics 9 (15) (2021) 1799.
[51] Laurent Gosse, A well-balanced scheme using non-conservative products designed for hyperbolic systems of conservation laws with source terms, Math. Models Methods Appl. Sci. 11 (June 1999).
[52] Laurent Gosse, A well-balanced flux-vector splitting scheme designed for hyperbolic systems of conservation laws with source terms, Comput. Math. Appl. 39 (May 2000) 135–159.
[53] Laurent Gosse, Localization effects and measure source terms in numerical schemes for balance laws, Math. Comput. 71 (January 2002) 553–582.
[54] Sigal Gottlieb, Chi-Wang Shu, Eitan Tadmor, Strong stability-preserving high-order time discretization methods, SIAM Rev. 43 (1) (2001) 89–112.
[55] J.M. Greenberg, A.Y. Leroux, R. Baraille, A. Noussair, Analysis and approximation of conservation laws with source terms, SIAM J. Numer. Anal. 34 (5) (1997) 1980–2007.
[56] Joshua M. Greenberg, Alain-Yves LeRoux, A well-balanced scheme for the numerical processing of source terms in hyperbolic equations, SIAM J. Numer. Anal. 33 (1) (1996) 1–16.

[57] Luc Grosheintz-Laval, Roger Käppeli, Well-balanced finite volume schemes for nearly steady adiabatic flows, J. Comput. Phys. 423 (2020) 109805.
[58] Ernesto Guerrero Fernández, Cipriano Escalante, Manuel J. Castro, Well-balanced high-order discontinuous Galerkin methods for systems of balance laws, Mathematics 10 (1) (2022).
[59] Guanlan Huang, Yulong Xing, Tao Xiong, High order well-balanced asymptotic preserving finite difference WENO schemes for the shallow water equations in all Froude numbers, arXiv:2108.04463 [abs], 2021.
[60] Shi Jin, A steady-state capturing method for hyperbolic systems with geometrical source terms, ESAIM: Math. Model. Numer. Anal. (Modélisation Mathématique et Analyse Numérique) 35 (4) (2001) 631–645.
[61] Shi Jin, Asymptotic preserving (AP) schemes for multiscale kinetic and hyperbolic equations: a review, in: Lecture Notes for Summer School on Methods and Models of Kinetic Theory (M&MKT), Porto Ercole, Grosseto, Italy, 2010, pp. 177–216.
[62] Shi Jin, Zhouping Xin, The relaxation schemes for systems of conservation laws in arbitrary space dimensions, Commun. Pure Appl. Math. 48 (3) (1995) 235–276.
[63] Farah Kanbar, Rony Touma, Christian Klingenberg, Well-balanced central schemes for the one and two-dimensional Euler systems with gravity, Appl. Numer. Math. 156 (June 2020).
[64] Roger Käppeli, Siddhartha Mishra, A well-balanced finite volume scheme for the Euler equations with gravitation-the exact preservation of hydrostatic equilibrium with arbitrary entropy stratification, Astron. Astrophys. 587 (2016) A94.
[65] Christian Klingenberg, Gabriella Puppo, Matteo Semplice, Arbitrary order finite volume well-balanced schemes for the Euler equations with gravity, SIAM J. Sci. Comput. 41 (January 2019) A695–A721.
[66] Christian Klingenberg, Rony Touma, Ujjwal Koley, Well-balanced unstaggered central schemes for the Euler equations with gravitation, SIAM J. Sci. Comput. 38 (January 2016).
[67] Alexander Kurganov, Finite-volume schemes for shallow-water equations, Acta Numer. 27 (May 2018) 289–351.
[68] Alexander Kurganov, Guergana Petrova, A second-order well-balanced positivity preserving central-upwind scheme for the Saint-Venant system, Commun. Math. Sci. 5 (1) (2007) 133–160.
[69] R. Käppeli, S. Mishra, Well-balanced schemes for the Euler equations with gravitation, J. Comput. Phys. 259 (2014) 199–219.
[70] Haegyun Lee, Implicit discontinuous Galerkin scheme for shallow water equations, J. Mech. Sci. Technol. 33 (July 2019).
[71] R.J. LeVeque, Balancing source terms and flux gradients in high-resolution Godunov methods: the quasi-steady wave-propagation algorithm, J. Comput. Phys. 146 (1) (1998).
[72] Maria Lukacova-Medvidova, Sebastian Noelle, Marcus Kraft, Well-balanced finite volume evolution Galerkin methods for the shallow water equations, J. Comput. Phys. 221 (January 2007) 122–147.
[73] Fabian Miczek, Friedrich K. Röpke, Philip V.F. Edelmann, New numerical solver for flows at various Mach numbers, Astron. Astrophys. 576 (2015) A50.
[74] Gino Moretti, Mivhael Abbett, A time-dependent computational method for blunt body flows, AIAA J. 4 (12) (1966) 2136–2141.
[75] Lucas O. Müller, Carlos Parés, Eleuterio F. Toro, Well-balanced high-order numerical schemes for one-dimensional blood flow in vessels with varying mechanical properties, J. Comput. Phys. 242 (June 2013) 53–85.
[76] Sebastian Noelle, Normann Pankratz, Gabriella Puppo, Jostein Natvig, Well-balanced finite volume schemes of arbitrary order of accuracy for shallow water flows, J. Comput. Phys. 213 (April 2006) 474–499.
[77] Sebastian Noelle, Yulong Xing, Chi-Wang Shu, High-order well-balanced finite volume WENO schemes for shallow water equation with moving water, J. Comput. Phys. 226 (September 2007) 29–58.
[78] Lorenzo Pareschi, Giovanni Russo, Implicit–explicit Runge–Kutta schemes and applications to hyperbolic systems with relaxation, J. Sci. Comput. 25 (1) (2005) 129–155.
[79] Carlos Parés, Carlos Parés-Pulido, Well-balanced high-order finite difference methods for systems of balance laws, J. Comput. Phys. 425 (2021) 109880.
[80] Marica Pelanti, François Bouchut, Anne Mangeney, A Roe-type scheme for two-phase shallow granular flows over variable topography, ESAIM Math. Model. Numer. Anal. 42 (September 2008) 851–885.
[81] Benoît Perthame, Chiara Simeoni, A kinetic scheme for the Saint-Venant system with a source term, Calcolo 38 (November 2001) 201–231.
[82] Benoît Perthame, Chiara Simeoni, Convergence of the upwind interface source method for hyperbolic conservation laws, in: Hyperbolic Problems: Theory, Numerics, Applications, Springer, 2003, pp. 61–78.
[83] Mario Ricchiuto, An explicit residual based approach for shallow water flows, J. Comput. Phys. 280 (January 2015) 306–344.
[84] Mario Ricchiuto, Andreas Bollermann, Stabilized residual distribution for shallow water simulations, J. Comput. Phys. 228 (4) (March 2009) 1071–1115.
[85] P.L. Roe, Upwind differencing schemes for hyperbolic conservation laws with source terms, in: Claude Carasso, Denis Serre, Pierre-Arnaud Raviart (Eds.), Nonlinear Hyperbolic Problems, Springer Berlin Heidelberg, Berlin, Heidelberg, 1987, pp. 41–51.
[86] Giovanni Russo, Alexander Khe, High Order Well Balanced Schemes for Systems of Balance Laws, Proceedings of Symposia in Applied Mathematics, vol. 67, January 2009, pp. 919–928.
[87] Huazhong Tang, Tao Tang, Kun Xu, A gas-kinetic scheme for shallow-water equations with source terms, Z. Angew. Math. Phys. 55 (May 2004) 365–382.
[88] Maurizio Tavelli, Michael Dumbser, A high order semi-implicit discontinuous Galerkin method for the two dimensional shallow water equations on staggered unstructured meshes, Appl. Math. Comput. 234 (C) (May 2014) 623–644.
[89] R.S. Deepak Varma, Praveen Chandrashekar, A second-order well-balanced finite volume scheme for Euler equations with gravity, Comput. Fluids 181 (March 2018).
[90] Stefan Vater, Rupert Klein, A semi-implicit multiscale scheme for shallow water flows at low Froude number, Commun. Appl. Math. Comput. Sci. 13 (September 2018) 303–336.
[91] Yulong Xing, Chi-Wang Shu, High-order well-balanced finite difference WENO schemes for a class of hyperbolic systems with source terms, J. Sci. Comput. 27 (2006) 477–494.
[92] Yulong Xing, Chi-Wang Shu, High order well-balanced finite volume WENO schemes and discontinuous Galerkin methods for a class of hyperbolic systems with source terms, J. Comput. Phys. 214 (2006) 567.
[93] Lanhao Zhao, Bowen Guo, Tongchun Li, E.J. Avital, J.J.R. Williams, A well-balanced explicit/semi-implicit finite element scheme for shallow water equations in drying–wetting areas, Int. J. Numer. Methods Fluids 75 (12) (2014) 815–834.